Potential Contribution of Carbon Sequestration in the North Eastern Part of the Bay of Bengal Bangladesh

Raju Das

Roll No: 0122/07

Registration No: 1107

Session: 2022-2023

A thesis submitted in the partial fulfillment of the requirements for the degree of Master of Science in Marine Bioresource Science

Department of Marine Bioresource Science
Faculty of Fisheries
Chittagong Veterinary and Animal Sciences University
Chittagong-4225

December 2023

AUTHORIZATION

I hereby declare that I am the sole author of the thesis. I also authorize the Chattogram Veterinary and Animal Sciences University (CVASU) to lend this thesis to other institutions or individuals for the purpose of scholarly research. I further authorize the CVASU to reproduce the thesis by photocopying or by other means, in total or in part, at the request of other institutions or individuals for the purpose of scholarly research.

I, the undersigned, and author of this work, declare that the **electronic copy** of this thesis provided to the CVASU Library, is an accurate copy of the print thesis submitted, within the limits of the technology available.

The Author

December 2023

Potential Contribution of Carbon Sequestration in the Northeastern the Bay of Bengal, Bangladesh

Raju Das

Roll No. 0122/07

Registration No. 1107

Session: 2022-2023

This is to certify that we have examined the above Master's thesis and have found that is complete and satisfactory in all respects, and that all revisions required by the thesis examination committee have been made

----------	----------
-	-
Supervisor	**Co-supervisor**
Nayeema Ferdausy Hoque	**Dr. Md Asaduzzaman**
Assistant Professor	**Associate Professor**
Department of Marine Bioresource Science	**Department of Marine Bioresource Science**
Faculty of Fisheries, CVASU	**Faculty of Fisheries, CVASU**

Dr. Md Sadequr Rahman Khan
Chairman of the Examination Committee

Department of Marine Bioresource Science
Faculty of Fisheries
Chittagong Veterinary and Animal Sciences University
Khulshi, Chittagong-4225, Bangladesh

DECEMBER 2023

TABLE OF CONTENTS

LIST OF FIGURES

LIST OF TABLES

LIST OF ABBREVIATIONS

BoB	Bay of Bengal
MODIS	Moderate Resolution Imaging spectroradiometer
ArcGIS	Aeronautical Reconnaissance Coverage Geographic Information System
CF	Carbon Flux
TC	Total Carbon
PSR	Phytoplankton Sinking Rate
Chl-a	Chlorophyll-a
POC	Particulate Organic Carbon
PIC	Particulate Inorganic Carbon
mg	Milligram
m	Meter
kg	Kilogram
Gt	Gigatonne
GtC	Gigatonnes of Carbon
GEBCO	General Bathymetric Chart of the Oceans
NDVI	Normalized Difference Vegetation Index
VIIRS	Visible Infrared Imaging Radiometer Suite
CO_2	Carbon Dioxide
OC	Organic Carbon
IPCC	Intergovernmental Panel on Climate Change

Pg	Petagram
C	Carbon
pCO_2	Partial Pressure of Carbon Dioxide
UNESCO	United Nations Educational, Scientific and Cultural Organization
USGS	United States Geological survey
NaOH	Sodium Hydroxide
GPP	Gross Primary Productivity
NPP	Net Primary Productivity
O_3	Ozone
DOC	Dissolve Organic Carbon
SeaWIFS	Sea-viewing Wide Field-of-view Sensor
et al.	And Others
km	Kilometer
Sq	Square
cm	Centimeter
µg	Micrometer
l	Litre
NASA	National Aeronautics and Space Administration
OBPG	Ocean Biology Processing Group
nm	Nano meter
NOAA	National Oceanic and Atmospheric Administration

NE	North Eastern
SE	South Eastern
SNPP	Suomi National Polar-Orbiting Partnership
JPSS	Joint Polar Satellite System
e.g	Example
NEM	North-east Monsoon
CDM	Clean Development Mechanism
$CaCO_3$	Calcium Carbonate
MT	Metric ton
tC	Tons of Carbon
ha	Hectare
CHTs	Chittagong Hill Tracts
NW	North Western
SW	South Western
CCS	Carbon Capture and Storage
EEZ	Exclusive Economic Zone
SST	Seasonal Surface Temperature

ABSTRACT

This research delves into the critical study of carbon sequestration dynamics in the northeastern Bay of Bengal (BoB) with a focus on understanding the status, trends and influencing factors. A multifaceted approach encompassing both secondary satellite data and primary field observations was employed. Satellite data, sourced from platforms such as MODIS and others, were meticulously processed using ArcGIS modeling approaches tools. Concurrently, field observation data, encompassing parameters like Chlorophyll-a (Chl-a)concentration, Carbon Flux (CF), Total Carbon (TC) and Phytoplankton Sinking Rate (PSR) were collected, processed and analyzed to provide comprehensive insights of Carbon sequestration. The study highlight intriguing seasonal and annual variations in key parameters, notably Chl-a, Particulate Organic Carbon (POC) and Particulate Inorganic Carbon (PIC). Seasonal variations demonstrated distinct trends across different seasons, suggesting variations in carbon sequestration activities. Over a 3-years period (2009-10, 2014-15, 2019-20), the average surface POC concentration was 177.64±144.61 mgm^{-3} and PIC concentration was 0.05±0.13 mgm^{-3} in the northern Bay of Bengal (BoB). Specifically, increasing trends in winter and monsoon for POC and PIC imply enhanced carbon sequestration activities during these periods. Depth-wise variations further illuminated the influence of CF and total carbon emphasizing their significance in carbon sequestration dynamics. This pioneering study provides invaluable insights into the seasonal and annual trends of Chlorophyll-a, Total Carbon and Phytoplankton Sinking Rate in the Bay of Bengal region, bridging the gap between real-time data and MODIS satellite observations. The research underscores the substantial carbon sequestration potential of the northeastern BoB, particularly during the monsoon season. However, further research is imperative to refine MODIS data accuracy and explore the vertical and spatial profiles of carbon stock.

CHAPTER ONE: INTRODUCTION

1.1 Background study

Carbon sequestration is the long-term storage of carbon in living organisms, nonliving geological formations and the oceanic environment. The process of capturing and storing carbon in a carbon pool is basically known as carbon sequestration (Daggash, 2021). Natural biological, chemical, and physical processes remove carbon dioxide (CO_2) from the atmosphere. CO_2 is considered as a key greenhouse gas in the atmospheric biogeochemical cycle, which has potential impacts on climate change. This process of sequestration helps to mitigate or defer global warming and avoid dangerous global climate change (USGS, 2023). Both naturally and through human activities, carbon sequestration refers to the process of its storage. In response to the growing concern of climate change resulting from the increased level of atmospheric CO_2, considerable interest has been drawn to the possibility of increasing rate of CO_2 storage for long periods of time through land use pattern change and the geo-engineering techniques such as carbon capture and storage (Allenby, 2002).

Since the late 1800s, global surface temperatures have increased by 0.88°C, marking 11 of the 12 warmest years on record since 1995 (Haywood et al., 2007). Projections of the twenty-first century indicate a further temperature rise of approximately 1.5–5.9 degrees Celsius (Joos et al., 2001). The trend is linked to the escalating concentration of greenhouse gases particularly carbon dioxide (CO_2), stemming from industrial emissions and deforestation (Althoff and Chandler, 1999). Anticipated consequences include a rise in earth's average temperature. Addressing this issue, carbon sequestration involves the transfer of CO_2 from the atmosphere into enduring global reservoirs such as marine, soil, living organisms and geological formations (Lal et al., 2008). The ocean currently serves as the largest CO_2 sink in the atmosphere, absorbing approximately 7 Pg per year (Metz et al., 2005). Encompassing over 70% of the earth's surface and boasting an average depth of 3800 meters, the vastness of the oceans is substantial. Nevertheless, due to equilibrium with atmospheric CO_2, the dissolution of CO_2 is contributing to surface ocean acidification, particularly impacting the most productive regions of the ocean (Calderia et al., 2003). The oceans have absorbed almost one-third of human-generated CO_2 with the atmosphere retaining about 43%, while the seas have taken up about 30%. This absorption has led to a 0.1 unit decline in surface pH,

decreasing from 8.2 to 8.1. If CO_2 emissions persist without mitigation, it is projected that the subsurface ocean's total CO_2 content may decrease by 0.7 units by 2030. Over the next 500 years, estimates suggest that the total carbon added to the atmosphere could reach around 5000 PgC (petagrams of carbon), based on fossil fuel reserves excluding hydrates. This rate of carbon addition represents the fastest in earth's history over a relatively short geological time span (Aze et al., 2014).

In the world oceans, the Bay of Bengal is one of the few places where land, marine, and atmospheric systems interact actively. The Bay of Bengal is a positive water balance zone, meaning that rainfall and river runoff considerably outnumber evaporation, resulting in low surface salinities and strong stratification (Varkey et al., 1996). It receives a massive volume of freshwater from major rivers like the Ganges, Brahmaputra, Godavari, Mahanadi, Cauvery, Irrawaddy, and Krishna (1.61012 m^3/yr; UNESCO 1979) and high precipitation, which flows into the Bay of Bengal. Marine sediments are one of the planets largest and most important carbon (C) repositories, making them essential for controlling climate change. Despite the fact that less than 1% of global gross domestic product ends up in the ocean (Hedges and Kei., 1995; Burdige et al., 2007), if not distributed organic C buried in ocean sediments can persist there for thousands to millions of years (Mcleod et al., 2011; Estes et al., 2019). Large-scale degradation of marine habitats has sparked concern that without protection, marine sediments may become a large source of carbon dioxide (CO_2) (Pendleton et al., 2012; Lovelock et al., 2017)

During the pre-South West Monsoon and North East Monsoon periods, studies were undertaken in the Bay of Bengal to better understand nutrients (Rao et al., 1994) and the inorganic carbon system (George et al., 1994; Kumar et al., 1996). Surface waters are completely barren of nutrients due to substantial vertical stratification, although surface partial pressure of carbon dioxide (pCO_2) levels were typically smaller than atmospheric values during both pre-South West Monsoon and North East Monsoon season. Because of the quick sedimentation and mineral-organic matter interaction in the bay, the removal of particulate carbon from the water column is significantly faster (NODC). Despite the fact that they only account for 7.6% of the world's ocean surface area (Sverdrup et al., 1942), they

have a significant impact. They have a considerable impact on atmospheric CO_2 absorption (Tsunogai et al., 1999).

In marine sea weed farming, carbon sequestration is important. When seaweed reaches the deep ocean, it sequesters carbon and prevents it from interacting with the atmosphere for millennia. Seaweed grows in shallow and coastal locations and can transport considerable amounts of carbon there (Ortega et al., 2019). Research is being done on growing seaweed offshore with the intention of sinking it in the ocean's depths to trap carbon (Temple et al., 2021). According to one study, seaweed farms could sustainably produce 200 kg of fish per person per year for a population of 10 billion people, remove 53 gigatonnes of CO_2 from the atmosphere, and produce enough bio methane to meet Earth's equivalent demand for fossil fuel energy if they occupied 9 percent of the ocean (Tim et al., 2015). Increased carbon sequestration may result from natural iron fertilization events (such as the precipitation of iron-rich dust into ocean waters). When sperm whales consume fish and defecate, they bring iron from the deep water to the surface, acting as fertilization agents. It has been demonstrated that sperm whales improve the amounts of primary production and carbon export to the deep ocean by discharging iron-rich feces into the Southern Ocean's surface waters. Phytoplankton grows and absorbs more carbon from the atmosphere because of the iron-rich excrement. When phytoplankton dies, some of it sinks to the bottom of the ocean, carrying carbon from the atmosphere with it. Whaling has caused an extra 200,000 tons of carbon to remain in the atmosphere each year by lowering the number of sperm whales in the Southern Ocean (Lavery et al., 2010).

Significant scientific efforts have been made since 1977, when the first theory of direct ocean sequestration of CO_2 was proposed (Marchetti et al., 1977). However, for this balance to be attained organically, thousands of years would pass. The ocean's absorption capacity is much smaller despite the fact that it contains 39,000 Gt of carbon as carbonate and bicarbonate. 1000 Gt (Gigatonne) of additional carbon would already significantly alter ocean chemistry (Lackner et al., 2002). Despite these restrictions, it has been estimated that the oceans can store more than 100,000 trillion GtC (Gigatonnes of carbon) (Herzog et al., 1997). Only if alkalinity (such as NaOH) were supplied to the ocean to neutralize the carbonic acid would such figures be possible. Such alkalinity might have been produced by the calcareous oozes

at the ocean's bottom dissolving over thousands of years (Archer et al., 1997; Broecker et al., 1977; Hoffert et al., 1979). Numerous CO_2 injection techniques have been researched. One method is to dilute the dissolved CO_2 below the mixed layer, where carbon can be stored for a few decades to hundreds of years but with limited capacity. Another strategy is to create CO_2 lakes at the ocean's bottom. Because compressed CO_2 has a density greater than seawater below 2700 meters, it sinks to the bottom. Additionally, CO_2 will react with saltwater to create solid clathrate, an ice-like cage structure with around six water molecules for every molecule of CO_2 (Soolan et al., 2003). The cost of directly disposing of CO_2 in the oceans has been estimated to be between $1 and $6 per ton (Freund et al., 1997) and $5 and $15 (Herzog et al., 2003; Metz et al., 2005). Environmental worries about long-term, recurring problems with changing the ocean's chemistry and on the local consequences of low pH (as low as 4) and its impact on marine creatures are the principal barrier to the acceptability of ocean storage (e.g., stunting coral growth). Replacing one environmental issue with another does not help (Lackner et al., 2010).

An ecosystem's net carbon sequestration is determined using several variables (Gower et al., 2003). The varied group of organisms known as plankton float in the water column of freshwater and oceanic areas. They are divided into two categories: phytoplankton, which are microscopic plants, and zooplankton, which are microscopic animals. At the base of the marine food chain, phytoplankton act as primary producers, using photosynthesis to transform sunlight into organic matter. Due to their contributions to the microbial and biological carbon pumps, both phytoplankton and zooplankton play a crucial part in the carbon cycle of maritime settings. These pumps have an impact on the global carbon cycle and climate regulation by facilitating the movement, transformation, and sequestration of carbon between the atmosphere, surface ocean, and deep ocean layers. Carbon dioxide (CO_2) from the atmosphere is converted into organic carbon molecules by phytoplankton through the process of photosynthesis. In addition to producing organic matter and supporting higher trophic levels, this primary production serves as the foundation of the marine food web. A portion of the organic matter created by phytoplankton sinks as aggregates, fecal pellets, and marine snow to deeper ocean layers. Through physical mechanisms, zooplankton feeding, and gravity settling, this exported organic carbon is carried to the deep ocean. When organic

carbon reaches deeper ocean strata, it is either absorbed by deep-sea microorganisms or retained in sediments or converted into refractory organic matter. In the deep ocean, this sequestration supports sediment building, biogeochemical cycling, and long-term carbon storage. On the other hand Deep-sea microorganisms, such as bacteria and archaea, respire to produce carbon dioxide while consuming oxygen in the process of breaking down organic materials. By remineralizing organic carbon, this microbial breakdown releases nutrients and dissolved inorganic carbon into the deep ocean. Through activities like denitrification, sulfate reduction, methanogenesis, and anaerobic metabolism, microbes aid in the recycling of nutrients, the transformation of organic matter, and the biogeochemical cycling of substances. These microbial mechanisms link microbial communities to global biogeochemical cycles by influencing nutrient availability, redox reactions, and carbon fluxes in the deep ocean (Polimene et al., 2017).

Gross primary production (GPP), also known as carbon uptake, is the process by which plants absorbs carbon dioxide (CO_2) from the atmosphere and stores it in its leaves, roots, and woody structures. The CO_2 is changed into carbohydrates during photosynthesis, which plants employ to produce biomass. When plants oxidize carbohydrates for tissue growth, maintenance, and repair, CO_2 is released into the atmosphere (Koss et al., 2007). The leaf area index increases with annual precipitation and soil water-holding capacity (Koss et al., 2007). A plant's productivity is directly inversely correlated with the amount of foliage. The plant will decrease its ability to photosynthesize as a result of the water shortage, which will lower its capacity to absorb carbon. As a result, less carbon will be sequestered (Gower et al., 2001). Other factor nutrients also influencing the carbon sequestration. The highest concentrations of nutrients are found in a plant's foliage. In order to maximize carbon gain, plants often maximize carbon allocation. Plants devote greater biomass to their roots in infertile soils to increase nutrient uptake (Gower et al., 2003). Plants growing on fertilized land exhibit the highest amounts of carbon sequestration (Qian et al., 2003). Then Empirical investigations have shown that rising temperatures increase soil heterotrophic respiration and reduce the amount of carbon that the soil can absorb. As a result, the soil's capacity to store carbon would decline. The results of short-term trials don't support these hypotheses (Gower et al., 2003). Then age is a factor influencing the carbon sequestration too. Over a plant's

lifetime, carbon sequestration often declines. This is thought to be caused by a drop in NPP brought on by nutrient shortages and hydraulic restrictions (Gower et al., 2003). Numerous vegetation types, including forests and grasslands, exhibit this impact. In addition to the lower rates of carbon sequestration, plants typically distribute carbon among several tissue types (Howard et al., 2004). Recent research on CO_2 and O_3 has revealed these gases will have an impact on carbon sequestration. A greater amount of carbon is available for plants to absorb when atmospheric CO_2 levels are high. The way that plants will distribute this resource has been the subject of extensive investigation over the past ten years. According to recent studies (King et al., 2005), NPP has increased by about 20%. Ozone levels at ground level have increased along with CO_2 levels. NPP levels have decreased when paired with ozone.

There has carbon pump that play a role in the carbon sequestration. The biological pump and physical pump is a collection of activities that fix inorganic carbon (like carbon dioxide) into organic matter through photosynthesis before securing it away from the atmosphere, typically by transporting it into the deep ocean. This can be done by dissolved organic matter in surface waters downwelling, zooplankton migrating vertically, or passive sinking of particle organic matter. The biological pump has a substantial impact on the distribution of numerous different chemical components of ocean water in addition to concentrating carbon in the deep sea. Predicting the biological pump's overall capacity and efficiency in various locations and at various periods is of great importance (including in the future). The capacity and efficiency of the biological pump on local and regional scales are strongly influenced by the physical environment, the type of phytoplankton present, the activities of zooplankton, the presence of biominerals and clay minerals, and the structure of the food web, complicating attempts to represent the biological pump in models (Rocha et al., 2014).

In order to enable studies on ocean biogeochemistry and ecosystems, satellite-derived data records of POC in the surface ocean offer a way to estimate the size and potential presence of multi-year trends in POC stock on a global and basin scale (Allison et al., 2010; Gaurier et al., 2010; Stramska et al., 2009). It is possible to advance a methodology to diagnose POC fluxes, such as primary production, export to the Deep Ocean, and formations to DOC and DIC pools, and to limit the uncertainties of carbon budget by tracking the rates of change in

POC in the upper ocean using satellite measurements (Allison et al., 2010). For the estimation of phytoplankton carbon biomass and carbon-based primary production from satellite measurements, the total pool of POC in the upper ocean also offers crucial data and limits 9 (Behrenfeld et al., 2005; Behrenfeld et al., 2013; King et al., 2005). The creation and use of remote sensing algorithms to calculate particulate organic carbon (POC) concentrations [in mg m] over the early years of operation of the satellite mission of the Sea-viewing Wide Field-of-View Sensor, satellite observations of ocean color were made in surface waters (SeaWiFS). The first POC algorithm was created using field data from the Southern Ocean and was based on two empirical relationships connecting the ocean's spectral remote-sensing reflectance, $R_{rs}(\lambda)$, with the seawater's spectral backscattering coefficient, $b_{bp}(\lambda)$, and the particulate backscattering coefficient, $b_{bp}(\lambda)$, with POC (where is light wavelength in vacuum and was selected from the green spectral region in the first POC (Stramski et al., 1999). While satellite data products were used in the algorithm development, another category of algorithms was based on field measurements of POC and optical data that were not all gathered in situ or during the same field operations 9 (Gardner et al., 2006; Loisel et al., 2001). Increased efforts have also been made in recent years with a focus on POC algorithms for coastal areas (Hu et al., 2016; Le et al., 2017; Liu et al., 2015). Stramska and Stramski (2006) and Stramski et al. 2006) investigated a number of empirical algorithms in which POC is derived from measurements of $R_{rs}(\lambda)$ or from a combination of $R_{rs}(\lambda)$ and IOPs (especially the backscattering and beam attenuation coefficients in open ocean environments. These studies suggested that, given the field data available at the time, the algorithm based on the $R_{rs}(\lambda)$ blue-green band ratio is a suitable candidate for applications to the global ocean, where the vast majority of most open-ocean waters are typically characterized by relatively low surface POC extending to about 300 mgm^{-3}.

POC is currently produced by the NASA Ocean Biology Processing Group (OBPG) as a standard worldwide ocean color product that is derived from the empirical link between surface POC and the remote-sensing reflectance's blue-green band ratio. POC and $R_{rs}(\lambda)$ readings from the eastern South Pacific and Atlantic Oceans were used to develop the original version of this technique for the SeaWiFS band ratio of R_{rs} (443 nm)/R_{rs} (555 nm), which encompassed a range of surface POC from around 10 to 300 mgm^{-3}. (Stramski et al., 2008). The Moderate Resolution Imaging Spectroradiometer (MODIS) and Visible Infrared

Imaging Radiometer Suite (VIIRS) ocean color sensors both use this band-ratio method. NASA OBPG has also adopted it. Since the start of the SeaWiFS program in 1997, NASA has been using these algorithms. A combination of SeaWiFS and later ocean color missions, such as MODIS-Terra and MODIS-Aqua as parts of the NASA-centered Earth Observing System (EOS) and VIIRS as part of NOAA/NASA partnership missions of Suomi National Polar-Orbiting Partnership (SNPP) and Joint Polar Satellite System (JPSS), currently provides more than 20 years of continuous satellite data of the global POC product.

It is widely known that waters in many coastal regions inner estuaries are net polluted (e.g., Green et al., 2006; Dai et al., 2008; Sarma et al., 2012). Because of the enormous amount of terrestrial input, it is heterotrophic and organic carbon in the form of particles (POC). Takahalshi et al., 2009 discovered that the Bay of Bengal is a perennial sink for atmospheric CO_2 based on gridded measurement data in the entire ocean. Kumar et al., 1996 studied surface pCO_2 levels in the western Bay of Bengal during the pre-southwest (March-April) and northeast monsoon (NEM) (December, 1991) seasons and found that they were always lower than atmospheric values. Estimating country-level carbon stocks using statistically validated methods is required to achieve the entire carbon reduction potential (Mahmood, Siddique, & Akhter, 2016). Bangladesh, as a member to the Kyoto Protocol, requires precise estimates of current carbon stocks across the country in order to execute carbon trading CDM projects (Saatchi et al., 2011). Bangladesh needs to estimate carbon emissions in order to execute climate change mitigation measures (Miah & Shin, 2009; Saatchi et al., 2011). Researchers in Bangladesh have evaluated carbon reserves in various forms in various locations of the nation and built algometric models.

1.2 Significance of this study

The current study is aimed to investigate the level of carbon sequestration through the spatio-temporal variation in the organic and inorganic carbon level. This study determines the annual and seasonal variation of Particulate Organic Carbon (POC), Particulate Inorganic Carbon (PIC) and Chlorophyll-a (Chl-a) concentration. This concentration of PIC and Chl-a level will clarify the status of carbon in the Bay of Bengal region. The level of POC and Chl-a concentration also indicates productivity and PIC indicates net calcification rate. The POC and Chl-a concentration is related to nutrient concentration of this regions as well as primary

productivity level. Lee et al., 2020 and on the other hand the zone where there is ideal PIC concentration will have ideal calcium carbonate ($CaCO_3$) **(**Lee et al., 2020**)**. As a result, the rate of fish population and the marine organisms that make their protective shell will be higher in this zone. Many Fish Species are sensitive to ocean productivity and aggregate near oceans fronts which attract prey. So this study will play an important role in the field of fisheries of Bay of Bengal and this study provide an improved tools for the development of a Bay of Bengal data record of PIC and Chl-a by merging observations from multiple satellite ocean color missions and will be more helpful in future research opportunities in remote sensing and biogeochemical modeling. The dynamic marine ecology of the Bay of Bengal is shaped by a number of variables, including atmospheric conditions, oceanic currents, and riverine inputs. Researchers may map and quantify regions with high potential for sequestering carbon dioxide by using GIS methods. This allows them to identify hotspots and get insight into the underlying mechanisms that drive carbon sequestration in this location. Conservation and management plans can be influenced by the identification of regions with high potential for sequestering carbon. By safeguarding and improving the region's natural ecosystems, which serve as carbon sinks, we can lessen the effects of climate change while also maintaining biodiversity and ecosystem services. Policymakers and other stakeholders can learn from the results of this kind of study how crucial the northeastern Bay of Bengal is to the global carbon cycle. At the national and regional levels, it can have an impact on policy choices about climate change adaptation and mitigation, sustainable fisheries management, and marine conservation. Coastal communities can benefit from creating policies that are climate resilient by having a better understanding of the carbon sequestration potential in the northeastern Bay of Bengal. Communities can profit from increased coastline protection, better water quality, and sustainable livelihood options through the preservation and restoration of natural ecosystems that sequester carbon.

This study aimed to explore some significance research questions as:

- What the status and potential trends in POC stock on BoB?
- Does the seasonal variability exert any influence on the concentrations of POC and PIC?

- How sinking rate influence the carbon flux along the coastal and maritime environment?

1.3 Objectives of the Study:

The objective of this research is:

1. to determine the level of carbon sequestration along the coastal and maritime region of Chattogram.
2. to explore and specifying the level of carbon using modeling approaches.

CHAPTER TWO: REVIEW OF LITERATURE

In recent years, rising global carbon emissions have posed a hazard. Numerous pertinent studies are being carried out globally to obtain an understanding of the amount of carbon released into the atmosphere and the amount absorbed by various sources, including the food chain. The majority of research indicates that the earth is entering a precarious situation and that atmospheric carbon is the main cause of concern. Therefore, it is impossible to dispute the role that photosynthesis plays in the huge amount of carbon that plants and oceanic phytoplankton are able to collect from the atmosphere. Marine phytoplankton fixes about 50 Gt of carbon annually and performs almost half of the photosynthesis worldwide (Basu and Mackey, 2018). The mechanisms leading to the transport of sinking particles, mainly phytoplankton, control how much carbon is sequestrated into the deep ocean through the biological pump. To accurately predict future levels of CO_2 in the atmosphere, it is important to understand how the biological carbon pump responds to climate change (Passow and Carlson, 2012). Due to the growing CO_2 levels in the atmosphere, the oceans will undergo significant changes.

The forest held almost 90% of the carbon that was stored by the forest sector. Carbon was transported from forests to wood products through regular management. As a result of ongoing production, under the existing climatic circumstances, the simulated storage of forest carbon increased by 45 percent by the year 2100 and that of wood products by 320 percent. When the temperature rose by more than 2.5°C within 40 years, the storage of carbon in the forest increased but then began to drop (Timo et al. 1998). A rise in annual production directly correlates with an increase in forest biomass and, thus, a larger capacity for carbon sequestration. According to estimates, the carbon pool for Indian forests in 1995 was 2026.72 Mt. Woods and plantations may have been able to remove at least 0.125 Gt of CO_2 from the atmosphere in 1995, according to estimates of yearly carbon uptake increase (Lal et al. 1998).

In Bangladesh, reforestation plays a major role in carbon sequestration and the production of carbon credits. Additionally, it is anticipated that selling carbon credits in the carbon market

through Clean Development Mechanism (CDM) projects will bring in a sizable sum of money. the impact of forestry initiatives on sequestering carbon in Bangladesh, namely in the hilly Chittagong region, and ends by illustrating the potential for carbon trading. tree tissue in the forests of Bangladesh stored 92 tons of carbon per hectare (tC/ha), on average. The results also revealed a gross stock of 190 tC/ha in the plantations (Shin et al., 2007)

In order to meet the 1.5–2.0°C temperature rise target set forth in the Paris Agreement, ocean sequestration of atmospheric carbon dioxide is increasingly seen as a crucial climate mitigation method (Aricò et al., 2021; Pörtner et al., 2019). The sustained oceanic carbon sink is essential for meeting this aim since it absorbs 37% of CO_2 emissions from fossil fuels, or 25% of the total emissions caused by burning fossil fuels and changes in land use between 1850 and 2019 (Friedlingstein et al., 2020).

The development of allometric equations and forest carbon estimation accounted for more than half of the published studies. The use of multiple terminology and assumptions, as well as arbitrary combinations of parameters such as age, topography, season, slope, crown diameter, and so on, made comparing available studies difficult. Outside of the woods of Chittagong and the Sundarbans, the spatial distribution of reports showed a confined geographical emphasis. Surprisingly, there were no attempts to investigate carbon stocks in the Chittagong Hill Tracts (CHTs), which contain the majority of the country's pristine forest areas (Majumder et al. 2019).

The current rate and capacity of natural terrestrial and oceanic sinks are insufficient to absorb the entire projected amount of anthropogenic CO_2 emissions during the twenty-first century or until C-neutral energy sources become effective, even though these sinks are currently absorbing about 60% of the 8.6 Pg C yr K1 emitted. Adoption of RMPs for forestry, agricultural crops, and pastures, as well as conversion to wise land use, can increase the sink capacity of managed ecosystems (such as forests, soils, and wetlands). By adopting regulatory measures and identifying policy incentives, deliberate manipulation of biological processes can expedite the process of sequestering CO_2 (Rattan et al. 2008).

During the southwest monsoon, when the Bay of Bengal's western continental shelf experiences its greatest discharge (10050 km^2), observations with high spatial resolution

were made there indicated that the inorganic carbon components in surface water are mostly influenced by freshwater discharge waters. In comparison to the southwest, the northwestern (NW) had lower atmospheric pCO_2 values Southwestern (SW) Bay of Bengal coastline. Compared to air levels and the glacial river Ganges (500 matm), the pCO_2 levels in the peninsular rivers were an order of magnitude greater (5000–17000 matm). The SW region is more impacted by the discharge from peninsular rivers, whilst the NW zone is more impacted by the Ganges river discharge (Sarma et al., 2012).. The characteristics of the rivers that discharge water and the East India Coastal Current, which distributes discharged water along the coast, determine whether the shelf region is a source or sink of CO_2. Although the situation is briefly reversed during the northeast monsoon and the region acts as a sink, on an annual basis, the western Bay of Bengal acts as a source for atmospheric CO_2 than previously thought.

Carbon and nutrients can be both sources and sinks in the soil. Changes in the amount of carbon stored in soils and variations in the climate can have an impact on the fluxes of CO_2 into and out of the atmosphere. Some agricultural management techniques will result in the soil's net sequestration of carbon The Global Change and Terrestrial Ecosystems Soil Organic Matter Network data were used to evaluate the potential for carbon sequestration in Europe (GCTE SOMNET). To quantify changes in the total carbon stock of European soils, linear correlations between management techniques and yearly variations in soil organic carbon were created. Regional estimations of the practices' capacity to trap carbon are vital if policymakers are to design future land uses to reduce national CO_2 emissions. The potential for carbon sequestration in Europe was assessed using data from the Global Change and Terrestrial Ecosystems Soil Organic Matter Network (GCTE SOMNET). Using linear correlations between management practices and yearly variations in soil organic carbon, changes in the total carbon store of European soils were quantified (Falloon et al. 1998).

Carbon capture and storage (CCS), lays out a number of novel concepts for coal-fired power plants that do not emit carbon dioxide into the atmosphere, and discusses these concepts in the context of retrofitting existing power plants, in the development of advanced power plant designs, and in conjunction with sufficient carbon dioxide storage options. CCS may offer a solution to the climate change issue, but implementing this cutting-edge technology will be a

significant endeavor. The introduction of this revolutionary technology is a significant task, but CCS may offer a solution to the climate change issue (Lackner et al. 2010).

The estimation of particulate organic carbon (POC) content from satellite images of the global ocean is of great interest since it is important for marine biogeochemical cycles and ecosystems. A new set of empirical POC algorithms were developed for various satellite sensors in order to produce a worldwide multi-decadal data record of POC by combining observations from various satellite ocean color missions. A field dataset of concurrent POC and remote-sensing reflectance, $R_{rs}(\lambda)$, measurements in all major ocean basins, covering tropical, subtropical, and temperate latitudes as well as the northern and southern polar latitudes were gathered in preparation for the algorithm development. Using seven distinctly different algorithmic categories, each with a fundamentally different definition of an independent variable including $R_{rs}(\lambda)$, over seventy formulas were assessed for calculating POC from $R_{rs}(\lambda)$. Based on SeaWiFS and MODIS-Aqua observations, a preliminary examination of field-satellite matchup datasets reveals that hybrid algorithms perform better than the existing standard algorithms for both SeaWiFS and MODIS (Stramski et al. 2022).

Remote sensing and GIS techniques such image classification, vegetation index models, and estimation of above-ground biomass approaches are used to calculate carbon sequestration. Land use and land cover mapping were used for comparison and estimation of carbon sequestration that either increased or decreased. To monitor biophysical conditions and vegetation cover, indicators such as the spectrally based Normalized Difference Vegetation Index (NDVI) and other vegetation indices produced by RS platforms are frequently employed. These indices are only meant to improve the spectral fingerprints of plants and lessen the effects of soil reflectance and air attenuation. GIS data layers and NDVI values were adjusted in order to determine CO_2 sequestration in a particular location. The combination of biomass models with NDVI data has made it simpler to estimate carbon stocks in forest regions (Konda et al. 2017).

Rouf et al., (2021) examines the seasonal and annual variations of POC in the northern Bay of Bengal (BoB) of Bangladesh and its correlation with wind vector, sea surface temperature (SST), and chlorophyll-a (Chl-a). It also verifies satellite data with data from in situ measurements. The Chl-a, and SST level-3 data from the Moderate Resolution Imaging

Spectroradiometer (MODIS) Aqua satellite were used in this investigation. WindSat Polarimetric Radiometer satellite provided the wind vector data. The surface POC concentration in the northern BoB declined at a rate of -1.12 mgm^{-3} $year^{-1}$, with an annual average of 153.84±11.17 mgm^{-3} over an 18-year period (2002–2019). The concentration varied from 126.83 mgm^{-3} to 180.58 mgm^{-3}. The POC was lowest (136.56±36.24 mgm^{-3}) in the pre-monsoon (March–May) and greatest (181.80±22.34 mgm^{-3}) during the northeast monsoon (December–February). A statistically significant variation in POC was seen between the seasons ($F_{3, 202} = 18.09$; $p<0.05$). Seasonally and annually, there was a very weak negative association between the SST and while in the northern BoB, there was a large positive relationship between POC and Chl-a. POC was found to be low with southwesterly wind in the southwest and pre-monsoon and extremely conspicuous with northeasterly wind in the northeast and post-monsoon. The primary factors influencing POC variability were Chl-a, and wind speed for BoB.

CHAPTER THREE: METHODOLOGY

This current chapter comprehensively addresses the research technique employed to achieve the study's objectives, elucidating the decision-making process behind selecting data gathering methods. It provides insight into the selection of research locations, techniques and analytical methods utilized in this study. The theoretical framework includes a flow chart outlining the methods employed in this research.

3.1 Area of the study

Bangladesh's southern region encompasses the Bay of Bengal, with a total water area, including the Exclusive Economic Zone (EEZ), measuring 66,000 sq. km. The Exclusive Economic Zone stretches up to a line situated 200 nautical miles from the baseline, marked by geographic coordinates $20^0$28'32.2"N and $90^0$33'41.5"E. This area was selected due to its inclusion in the United Nations Convention on the Law of the Sea's definition of an area of maritime jurisdiction. The research region shown in Figure 1.

The Bay of Bengal (BoB) is the world's largest bay, or body of water. The seasonal reversal of monsoonal winds and the substantial freshwater discharge into the BoB create a unique environment for investigating processes in monsoon regimes (Shetye et al., 1996; Hood et al., 2015).

While there are few reports on the distribution of carbon characteristics from BoB's oceanic waters, there have been few studies conducted in the coastal areas (Kumar et al., 1996). A special setting for researching biogeochemical processes in monsoon regimes is provided by the seasonal reversal of monsoonal winds and the significant freshwater discharge into the Bay of Bengal (BoB) (Shetye et al., 1996, Hood et al., 2015). The northeast (NE) coastline BoB had higher atmospheric pCO_2 values than the southwest (SE) coastal BoB. Nonetheless, compared to air levels and the glacial Ganges river (about 500 µatm), the pCO_2 levels in the peninsular rivers were an order of magnitude greater (5000–17,000 µatm) (Shetye et al., 1996).

For this study, locations in the northeast part, including Bashbaria, Patenga, Kutubdia, Cox's Bazar and Teknaf were selected. The selection of these stations was based on their proximity to the Bay of Bengal and samples were collected from a total twelve stations (Fig.2).

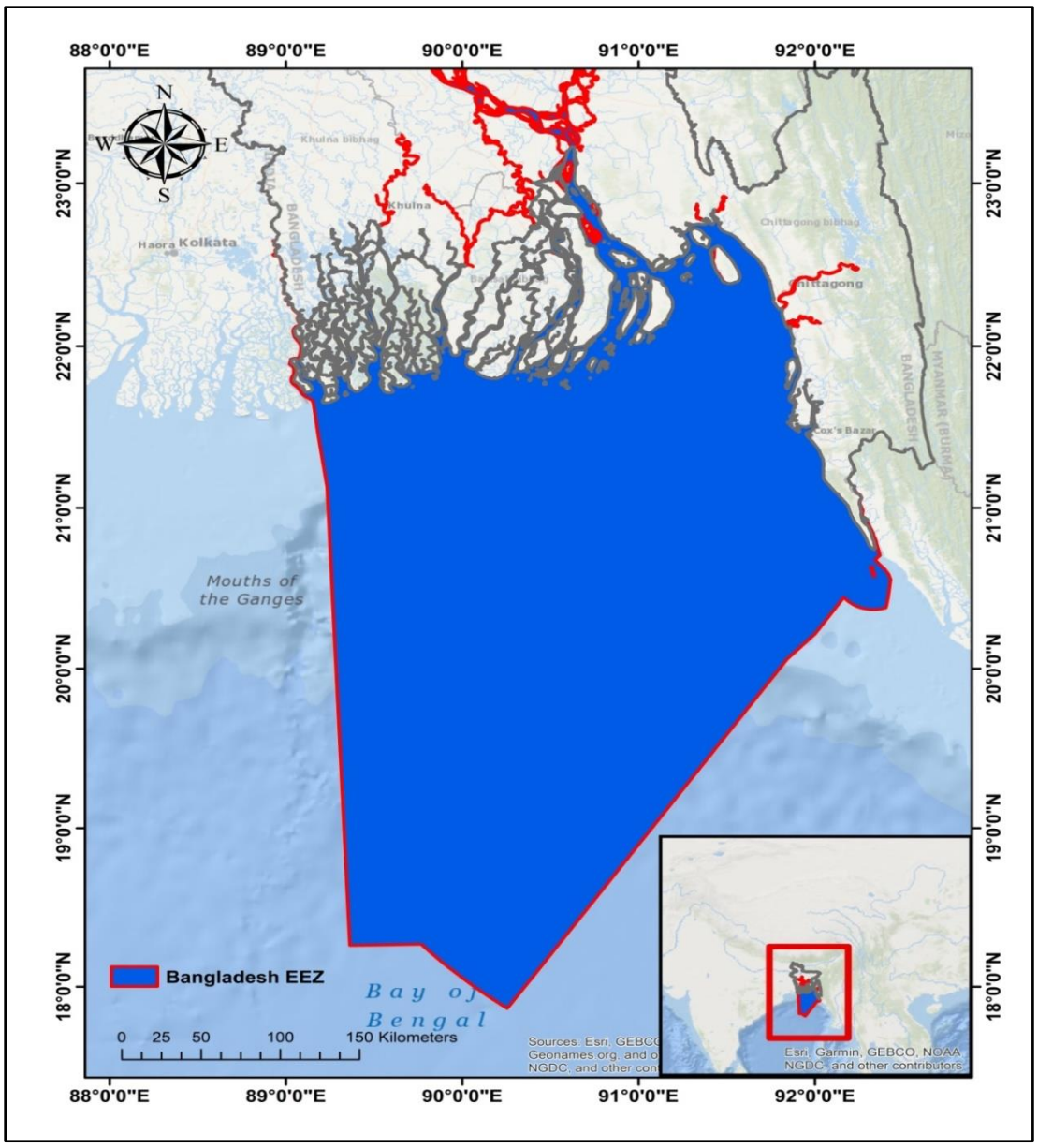

Fig. 1 *Study area map within Bangladesh EEZ Area*

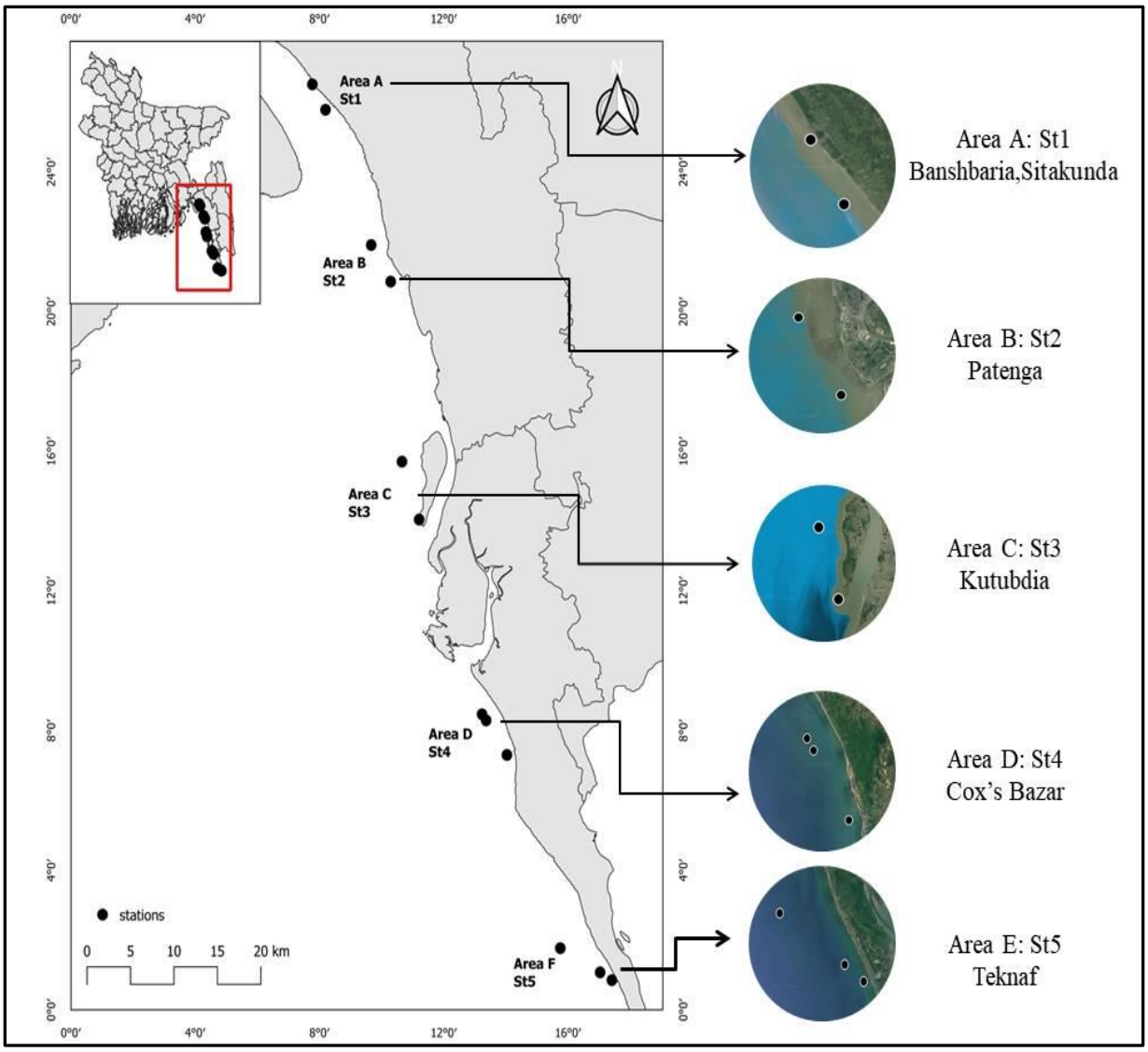

Fig. 2 *Main map and location of the study area in north eastern Bay of Bengal, Bangladesh*

Additionally, this study illustrates the data analysis techniques, encompassing model validation, graphical representations and data analysis itself, as depicted in Fig. 3.

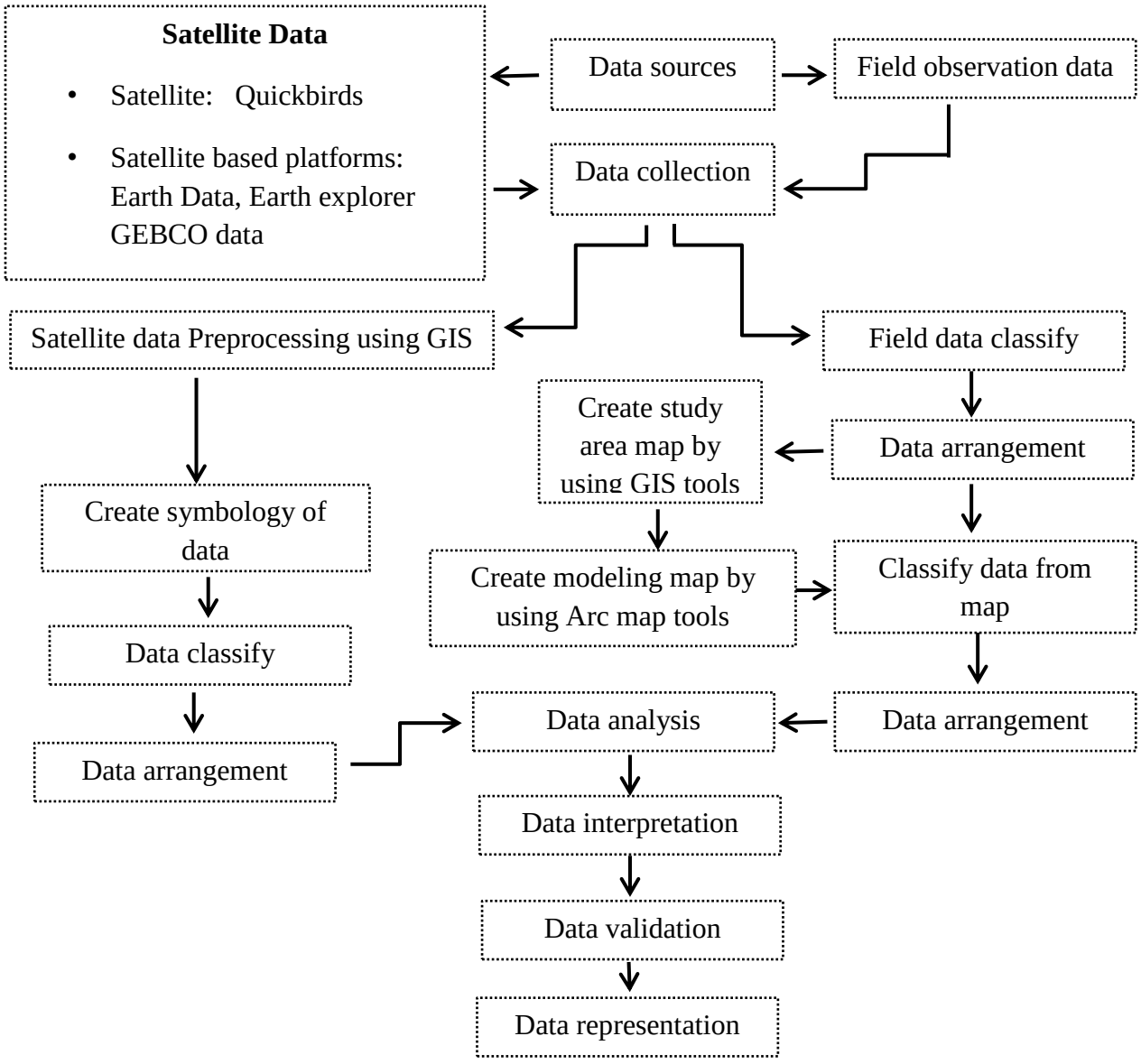

Fig. 3 *Flow diagram of the research procedure*

3.2 Data collection and pre-processing

Two types of sources were utilized for data collection during this research as satellite data (secondary data) and field observation data (secondary data). The satellite data sources include Quickbirds, Earth Data, Earth explorer and GEBCO data.

This study incorporates secondary data, sourced from both field observations and satellite based secondary data. Specially, the satellite data is derived from NASA Ocean color, known as MODIS data. MODIS-Aqua monthly and annual L3 Chlorophyll-a, Particulate Organic carbon (POC) and Particulate Inorganic Carbon (PIC) 4km resolution data were retrieved from NASA OBPG (Ocean Biology Processing Group) website (http://oceancolor.gsfc.nasa.gov/) for the four seasons- winter (Dec-Feb), pre-monsoon (Mar-May), monsoon (Jun-Aug), post-monsoon (Sep-Nov) during 2009-2010, 2014-2015, 2019-2020. Here, level-3 data was used because it has the highest level processing that is available and do not need the processing code. The moderate Resolution Imaging Spectroradiometer (MODIS) has 36 spectral band and 8-16 bands measure ocean color (Table.1) (MODIS Web). CI algorithm used by MODIS-Aqua sensor to retrieve chlorophyll. This OCI algorithm is combined from of two algorithms, one is CI based (reflectance difference-based) another is OCx based (reflectance ratio-based) algorithm, based on the CI-derived chl-a concentrations between 0.25 and 0.3 mg/m^3 (C. Hu et al., 2012).

$$CI=R_{rs}(\lambda_{green}) - [R_{rs}(\lambda_{blue}) + (\lambda_{green} - \lambda_{blue}) / (\lambda_{red} - \lambda_{blue}) * (R_{rs}(\lambda_{red}) - R_{rs}(\lambda_{blue}))]$$

Where, λ_{blue}, λ_{green} and λ_{red} are the instrument-specific wavelengths closet to 443,555 and 670nm respectively.

Table 1 *MODIS instrument specification for ocean color*

Band	Bandwidth (nm)	Spectral radiance
8	405-420	44.9
9	438-448	41.9

10	483-493	32.1
11	526-536	27.9
12	546-556	21.0
13	662-672	9.5
14	673-683	8.7
15	743-753	10.2
16	862-877	6.2

Here the format of MODIS data files are specified and the conversion steps are explained. All of the data, including coordinate systems, projections, and any georeferencing metadata present in the dataset, is georeferenced and filtered the information to concentrate on particular interest areas and metadata was documented to facilitate reproducibility and data understanding.

On the other hand field observation data is taken from a recent study and from this study I have taken four parameters of data. The parameters are: Chlorophyll-a concentration, Carbon Flux (CF), Total Carbon (TC) and Phytoplankton Sinking Rate (PSR). Here, outliers were detected and handled of these data and correct errors in the data are identified and corrected. Data sources were clearly identified for aggregation and this includes spreadsheets, databases, application programming interfaces, and other data repositories. Attention was paid to different data types (numeric, categorical, text) and consistency was ensure and converted data types to align them across sources. Determined which common keys were utilized to connect records from various databases.

3.3 Data processing through Arc GIS Modeling approaches

In this study Arc map (version 10.5) was used for modeling. ArcGIS offers a robust framework for modeling and analysis of geographic information systems (GIS). ArcGIS modeling approaches entail the processing and analysis of spatial data through the use of tools, functions, and processes. The spatial data was arranged and produced with care. This calls for the data to be cleaned, georeferenced, and validated. To develop, modify, and maintain geoprocessing models, ArcGIS's Model Builder tools were used. Through the use

of this graphical interface, geoprocessing tool connections can be visually designed as a workflow. The Spatial Analyst extension in ARC GIS uses one of several interpolation algorithms to produce a surface grid. The process of interpolation is utilized to forecast the values of cells in locations without sampled points. Its foundation is the principle of spatial dependence, also known as autocorrelation, which quantifies the degree of dependence or linkages between nearby and far-off items. To find out if values are connected, should use spatial autocorrelation. A spatial pattern is determined by how values are related to one another. The following is measured using this correlation:

- The degree of spatial correlation between a phenomenon and itself in space
- The degree of similarity between items within a region, and
- The degree of interdependence between the variables The character and degree of the dependency

A number of interpolation methods are available in Arc GIS Spatial Analyst version 10.5 to create surface grids from point data. The Spline, and kriging interpolation methods that were available in Arc Map 10.5 have been supplemented with the PointInterp, Natural Neighbors, and Trend methods as well as the Topo to Raster command. The distribution of sample points and the phenomenon under study will determine the best approach. Here I used Topo to Raster interpolation. The Topo to Raster approach ensures a hydrologically correct digital elevation model with a connected drainage system and accurate representations of ridges and streams from input contour data by interpolating elevation values for a raster. It makes use of an iterative finite difference interpolation method that preserves the surface continuity of the global interpolation while optimizing the computational efficiency of the local interpolation. It was created expressly to function sensibly when given contour inputs.

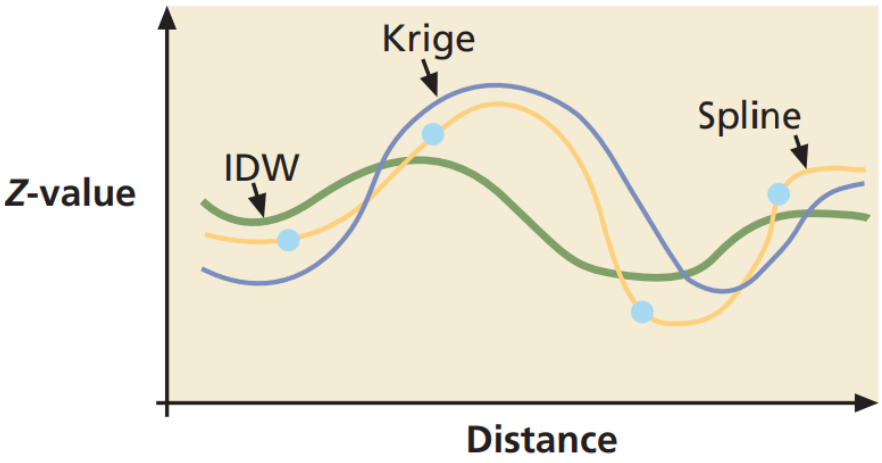

Fig. 4 *Two deterministic techniques that generate surfaces from samples depending on the degree of smoothing or similarity are IDW and Spline.*

3.4 Satellite data processing:

Data processing of remotely sensed satellite data normally involves the processing of digital images to improve the brightness value magnitudes (Shawal et al., 2014). The pre-processing image's main purpose is to reduce the influence of errors or inconsistencies in image brightness values that may limit one's ability to interpret or quantitatively process and analyze digital remotely sensed satellite images (Toutin et al., 2004). Here the data is processed by QGIS and Arc GIS tools. Geometric correction has been done to place the data correctly. Data from MODIS data sensors are available at several geographical and temporal resolutions. Pre-processing the dataset via a plug-in is required in order to use these datasets effectively in open-source GIS software such as QGIS. The QGIS plug-in is constructed with Python and the PyQt interface. The plug-in computerizes and processes the functionalities for MODIS products, such as MOD11, MOD09, and MOD21, based on MODIS Data (Terra/Aqua/Combined) (Toutin et al., 2004). Here symbols were selected from a style to represent features, elements, or visuals on map. Every symbol that is utilized is replicated and included into the map; no citation to the original style is kept. This implies that changing symbols on map won't affect the original styles from which they originated. Likewise, modifications made to a style's symbol won't show up on any maps that might use it and stored the modified symbol in a style after making changes to a symbol on map. The Style Manager Dialog box allows easily editing and saving symbols in a style. A typical procedure

was to copy symbols from an ArcGIS-installed read-only style, paste into a custom style, and then adjust the symbol properties as needed.

3.5 Ocean Data View

Ocean Data View (ODV) is a potent software program used in oceanography for data visualization and analysis. It is used for Data Visualization (multidimensional plots, contour plots, sectional plots), Data analysis (statistical analysis), Data interpolation, Metadata handling. In secondary data were imported. To load the data into the software, follow the prompts and enter the data in any format, including net and other supported file types. After the data was loaded, it was examined using where users may browse sections, profiles, and maps to gain a sense of the dataset. ODV provides a number of options, such as contour plots, line plots, scatter plots, and more. The study used scatter plots and customized these plots' appearances to improve their visual depiction. ODV allows creating multiple plots within the same session. Experimented with different plots and arrangements to gain comprehensive insights into data

CHAPTER FOUR: RESULT

In this chapter, the intricate facets of carbon sequestration are unraveled, delineating distinctions between particulate organic and inorganic carbon. The exploration extends to the ebb and flow of seasons, exploring their influence on sequestration dynamics within a spatial context. The chapter culminates in revealing through a satellite-based panoramic scrutiny and an introspective analysis of contemporaneous data from two antecedent theses.

4.1 Satellite-based measurements

4.1.1 Primary productivity (Chlorophyll-a)

Primary productivity refers to the rate at which energy is converted by photosynthetic organisms into organic substances. The concentration of chlorophyll-a in the water is often used as an indirect measure of the abundance of phytoplankton and by extension, an indicator of primary productivity. A seasonal time series of surface water Chlorophyll-a data was extracted from MODIS satellite imagery spanning three distinct years (2009-2010, 2014-2015 and 2019-2020). The surface Chl-a concentration within the Bangladesh EEZ over this triennial period unveiled intricate fluctuation in chlorophyll levels. The seasonal and annual composites of MODIS images provide an added perspective on the spatial distribution of chlorophyll-a (Chl-a) in the northern BoB from 2009 and 2020 (Fig 5).

With the incorporation of the appropriate season, the most productive zone was found in the post-monsoon with the concentration of 1.58 ± 2.17 mgm^{-3} and moderately zone found in the winter with 1.38 ± 1.66 mgm^{-3} concentration and lower productive zone found in the pre-monsoon with 2.07 ± 5.11 mgm^{-3} concentration in 2009-10 (Fig. 5)

In 2014-15, highly productive zone found in the pre-monsoon with 1.18 ± 1.61 mgm^{-3} and about moderately productive zone identified during the winter with 1.32 ± 1.66 mgm^{-3} concentration then lower productive zone also found in the winter (Fig. 5).

Then in 2019-2020, monsoon show the most productive zone with 2.56 ± 3.32 mgm^{-3} concentration and moderately productive zone found during the winter season) and lower productive zone found in the post-monsoon with the concentration of 3.58 ± 4.77 mgm^{-3} (Fig. 5).

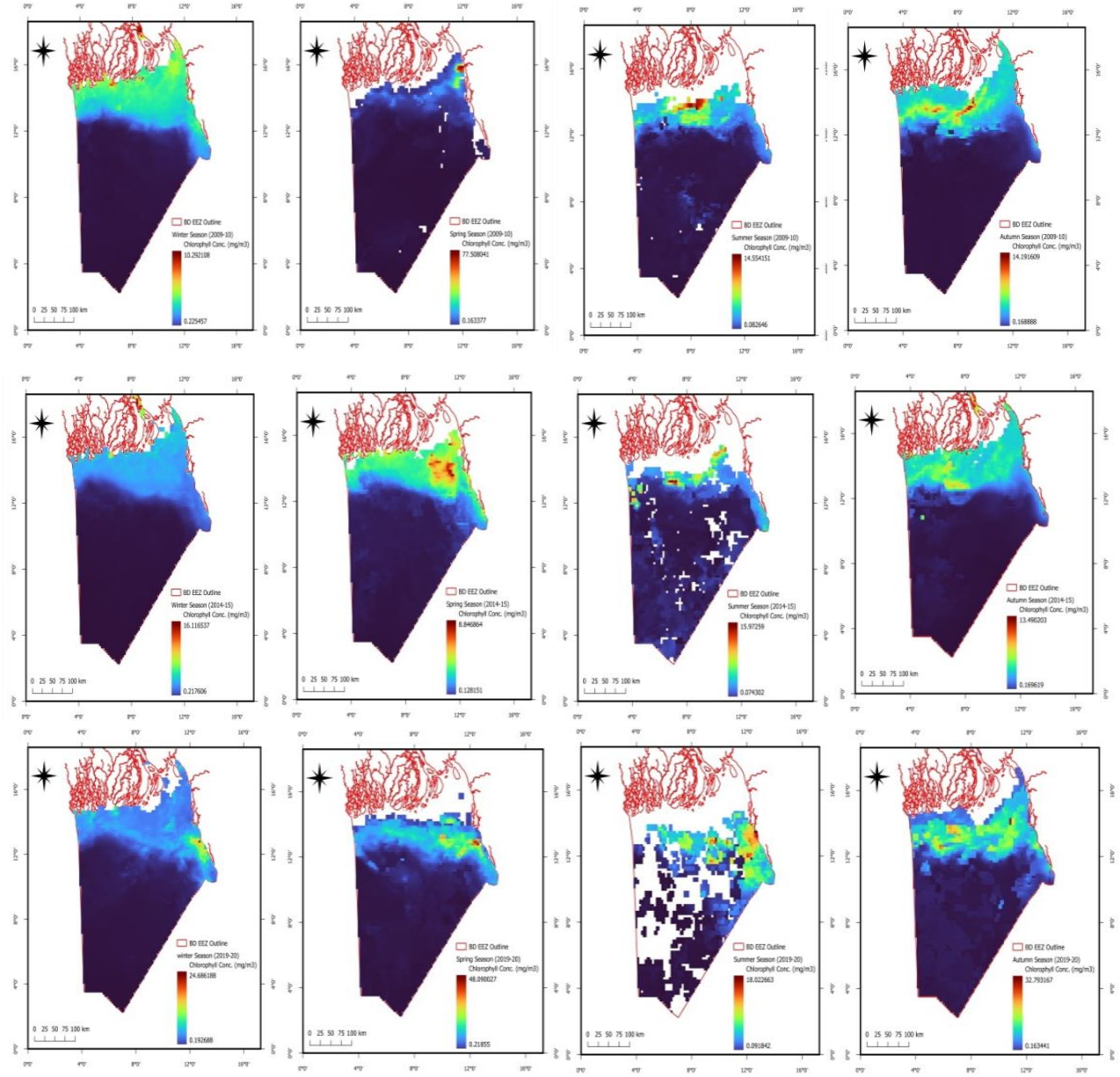

Fig. 5 *MODIS-derived Annual and Seasonal climatological Chl-a images from December 2009 - December 2020 in the Bangladesh EEZ*

The EEZ of this study area were categorized into highly productive, moderately productive less productive regions. The local seasons including winter, pre-monsoon, monsoon and post-

monsoon are denoted as winter, spring, summer and autumn in this MODIS data analysis and interpretation. During winter the highly productive zone occupied 7.71% in 2009-10 which reduced to 5.37%, 1.72% during 2014-15 and 2019-20 respectively. Then in spring the very productive zone was at 1.09% and it increased to 13.9% by 2014–15 and gradually decreased to 6.59% by 2019–20. The summer season shows the most productive zone at 6.24% in 2009-10 which progressively dropped to 5.39% in 2014-15 and again apexed to 16% in 2019-20. On the other hand, in 2009–10, the highly productive zone covered 12.5% of the area, by 2014–15 and 2019-20, that percentage dropped to 11.3%, and 10.12% respectively during autumn (Fig. 6).

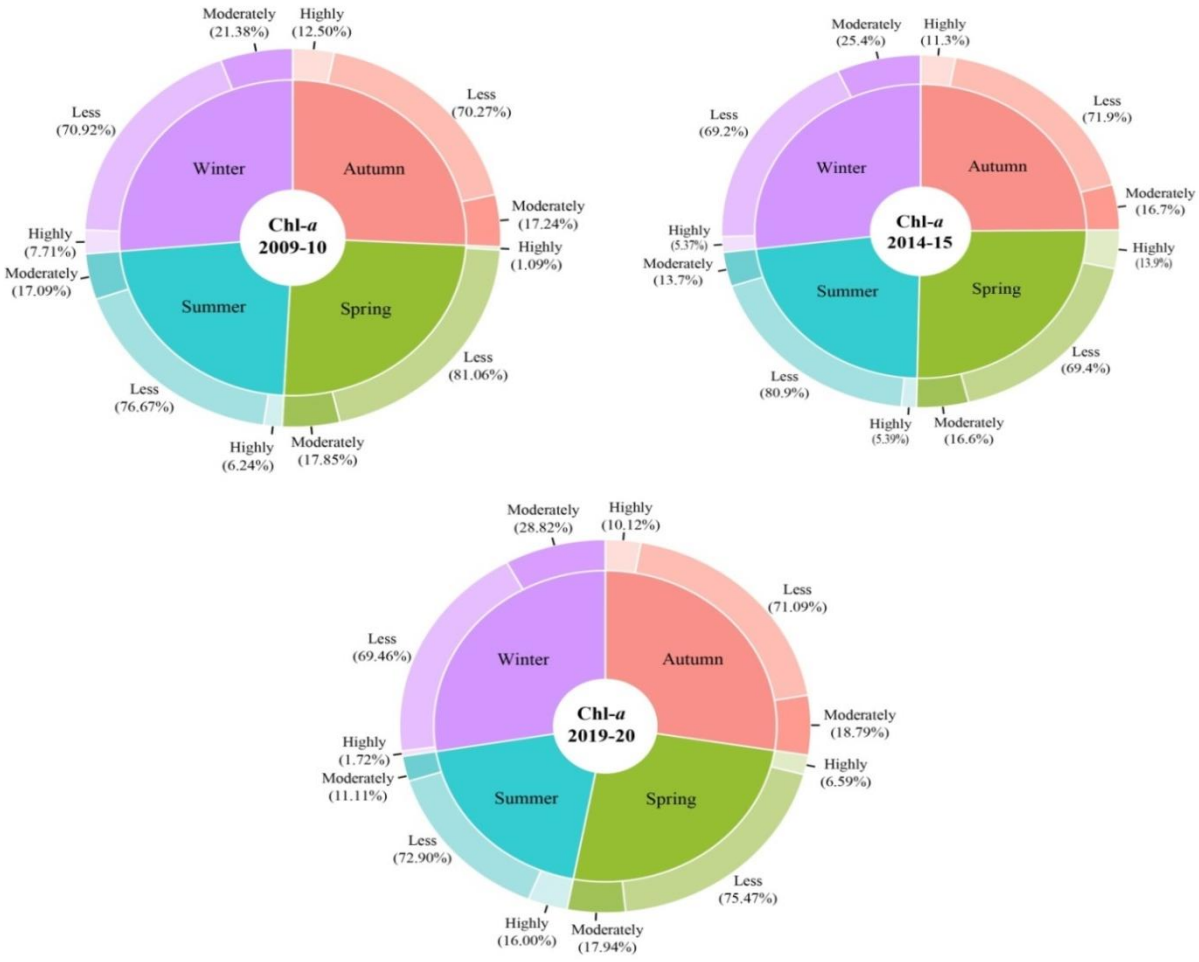

Fig. 6 *Percentage of annual and seasonal productivity in Chl-a concentration in the EEZ are of the Bay of Bengal over three years categorized as highly productive, moderately productive and less productive.*

4.1.2 Particulate Organic Carbon Variability

The annual trend provides a representation of the substantial and enduring fluctuations in particulate organic carbon (POC). The MODIS images' season and annual composites additionally illustrate the distribution of POC in the northern BoB between 2009 and 2020 (Fig 3).

After integration of respective month of specific season, about 23668.5 km^2 were identified as the most productive zone during the post-monsoon season (Sep-Nov) with 178.8 ± 160.8 mgm^{-3}, about 25391.5 km^2 were identified as moderately productive zone during the Pre-monsoon (Mar-May) with 226.1 ± 187.6 mgm^{-3} and about 63046.2 km^2 region were identified as lower productive zone during the post-monsoon (Sep-Nov) with 178.8 ± 160.8 mgm^{-3} concentration and averagely highest concentration was found in the spring season (Mar-May) (226.1 ± 187.6 mgm^{-3}) in 2009-2010 (Fig. 7).

On the other hand, in 2014-2015, about 24166.7 km^2 area was identified as the highest productive zone during the pre-monsoon with 151.6 ± 131.9 mgm^{-3}, about 20762.04 km^2 area was identified as the moderately productive zone during the winter with the concentration of 175.3 ± 142.1 mgm^{-3} and about 64712.6 km^2 area was identified as lower productive zone during the post-monsoon with 177.6 ± 157.1 mgm^{-3} (Fig. 7).

In 2019-20, there were about 26990 km^2 area higher productive zone during the post-monsoon season (Sep-Nov), about 12498.9 km^2 area was identified as moderately productive zone during the monsoon season (Jun-Aug) and about 60383.1km^2 area was identified as lower productive zone during the pre-monsoon season (Mar-May) and averagely the highest concentration was found in the winter season (Dec-Feb) with the POC concentration of 231 ± 156.8 mgm^{-3} (Fig. 7)

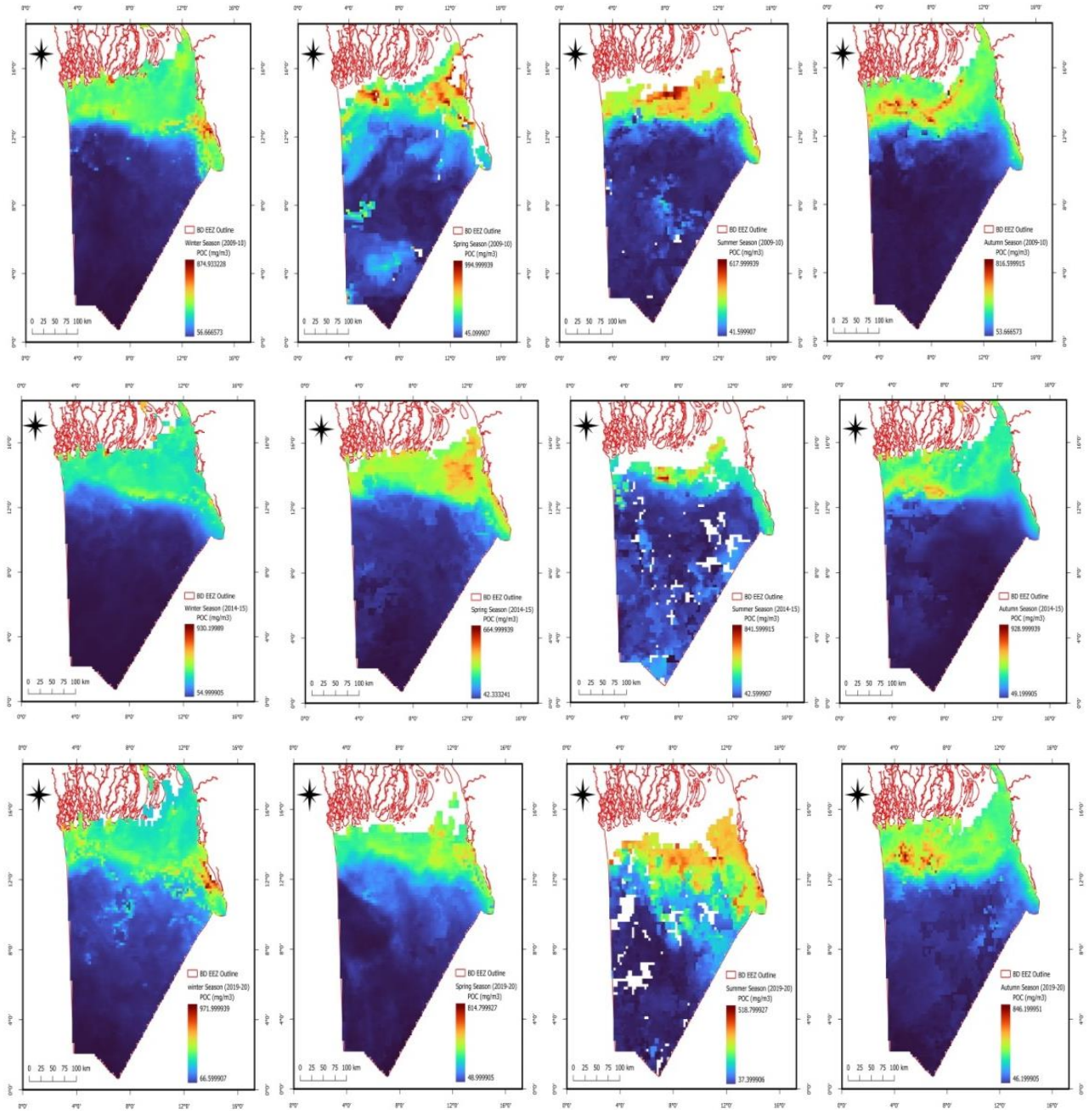

Fig. 7 *MODIS-derived Annual and Seasonal climatological POC images from December 2009 - December 2020 in the Bangladesh EEZ*

For clarity in MODIS data analysis and interpretation, the local season- winter, pre-monsoon, monsoon and post-monsoon are represented as winter, spring, summer and autumn season respectively. The extremely productive zone accounted for 24.19% of total production in 2009–10 and this percentage fell to 10.73% and apexed to 27.07% during winter in 2014-15 and 2019-20 respectively. In spring, the zone's productivity started at 19.49% in 2009-10, surged to 26.44% by 2014-15 and then tapered to 21.44% by 2019-20. For the summer, the peak productivity was 20.93% in 2009-10; this declined to 9.4% by 2014-15 and then rose to 33.14% by 2019-20. Contrarily, during autumn, the highly productive zone covered 24.41% in 2009-10, by 2014-15, this proportion dwindled to 19.66% and again fluctuated to 28.05 (Fig. 8).

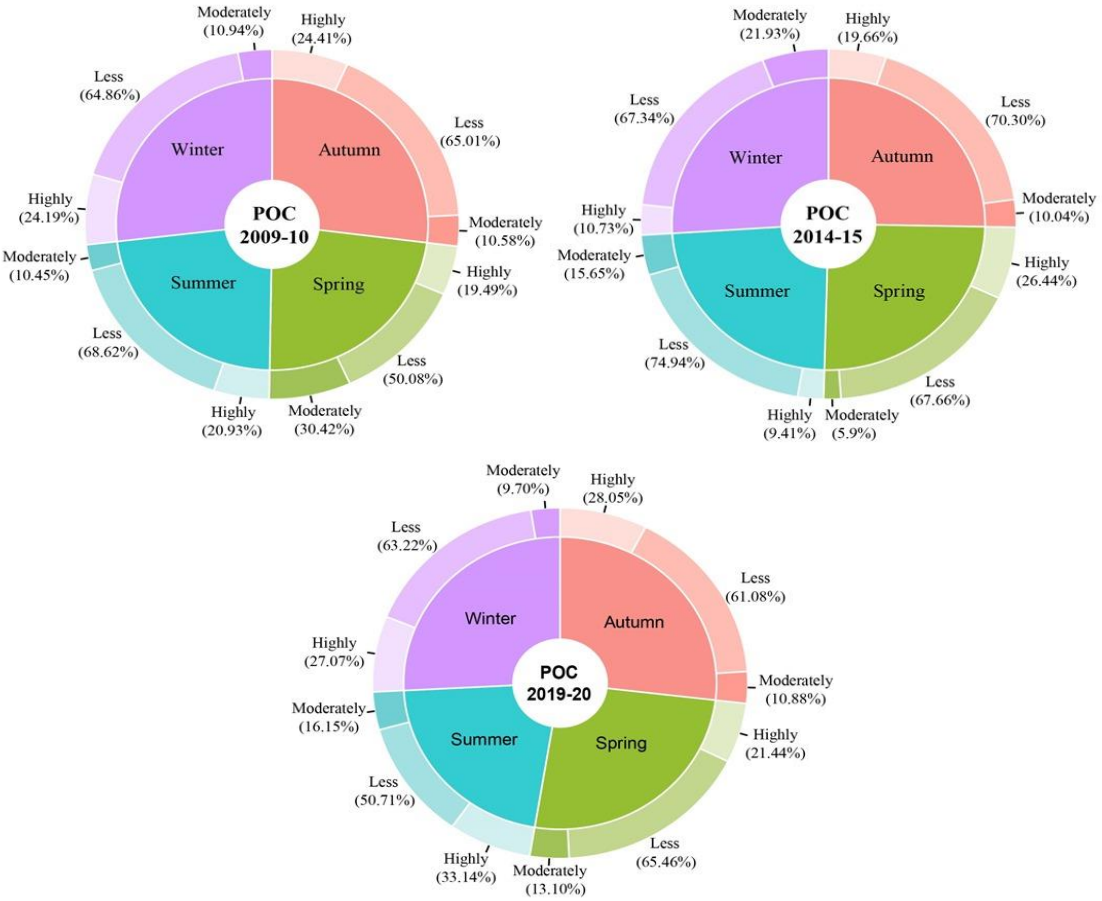

‘’’

Fig. 8 *Percentage of yearly and seasonal productivity according to POC concentration in the EEZ are of the Bay of Bengal over three years categorized as highly productive, moderately productive and less productive.*

4.1.3 Particulate Inorganic Carbon Concentration:

PIC was also observed in the surface PIC concentration in the Bangladesh EEZ.

In 2009-2010, here also identified high, moderate and low productive zone according to season. These are followed as post-monsoon (0.002 ± 0.008 mgm^{-3}), monsoon ($0.003 \pm 0.011 mgm^{-3}$) and post-monsoon and in 2014-2015 most productive zone identified during winter (0.58 ± 1.34 mgm^{-3}) whereas 2019-2020 shows monsoon (0.003 ± 0.009 mgm^{-3}) as the highest productive zone and winter as the lowest productive zone (Fig. 9)

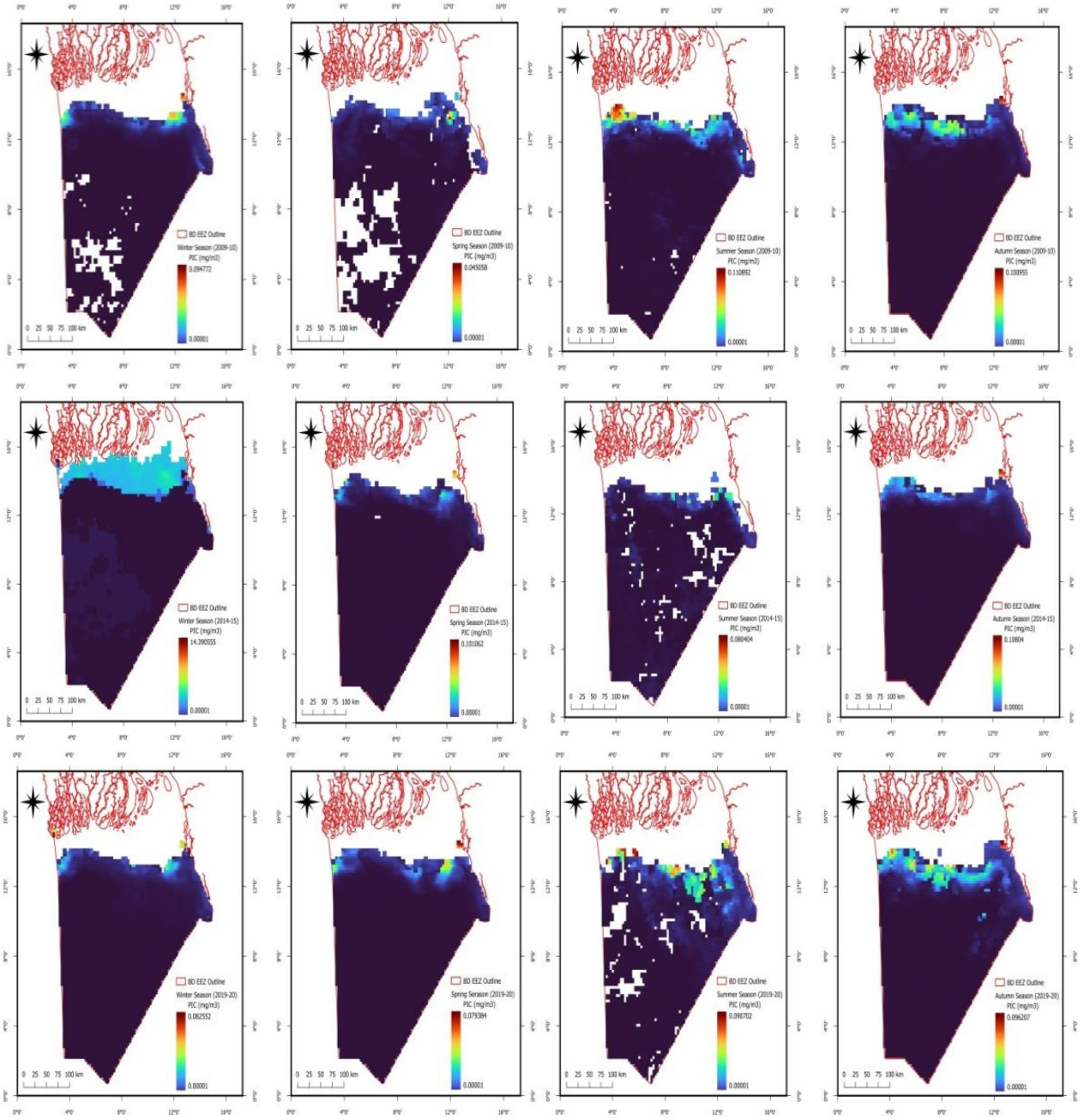

Fig. 9 *MODIS-derived Annual and Seasonal climatological PIC images from December 2009 - December 2020 in the Bangladesh EEZ*

Over the winter of 2009–10, the particularly productive zone generated 1.89% of the total crop. This percentage decreased to 0.26% by 2014–15, but again increased to 0.46% by

2019–20. Moving to spring, the productivity of this zone began at 0.38% in 2009-10, reduced to 0.26%by 2014-15 and then peaked to 0.86%. For summer, the peak productivity recorded ws 1.79% in 2009-10, however, this declined to 0.19% by 2014-15 and apexed to 2.59% by 2019-20. Conversely, in 2009–10, the very productive zone contributed for 2.26% of total production during the winter. This percentage dropped to 0.29% by 2014–15, but it subsequently rose significantly to 1.97% by 2019–20 (Fig. 10).

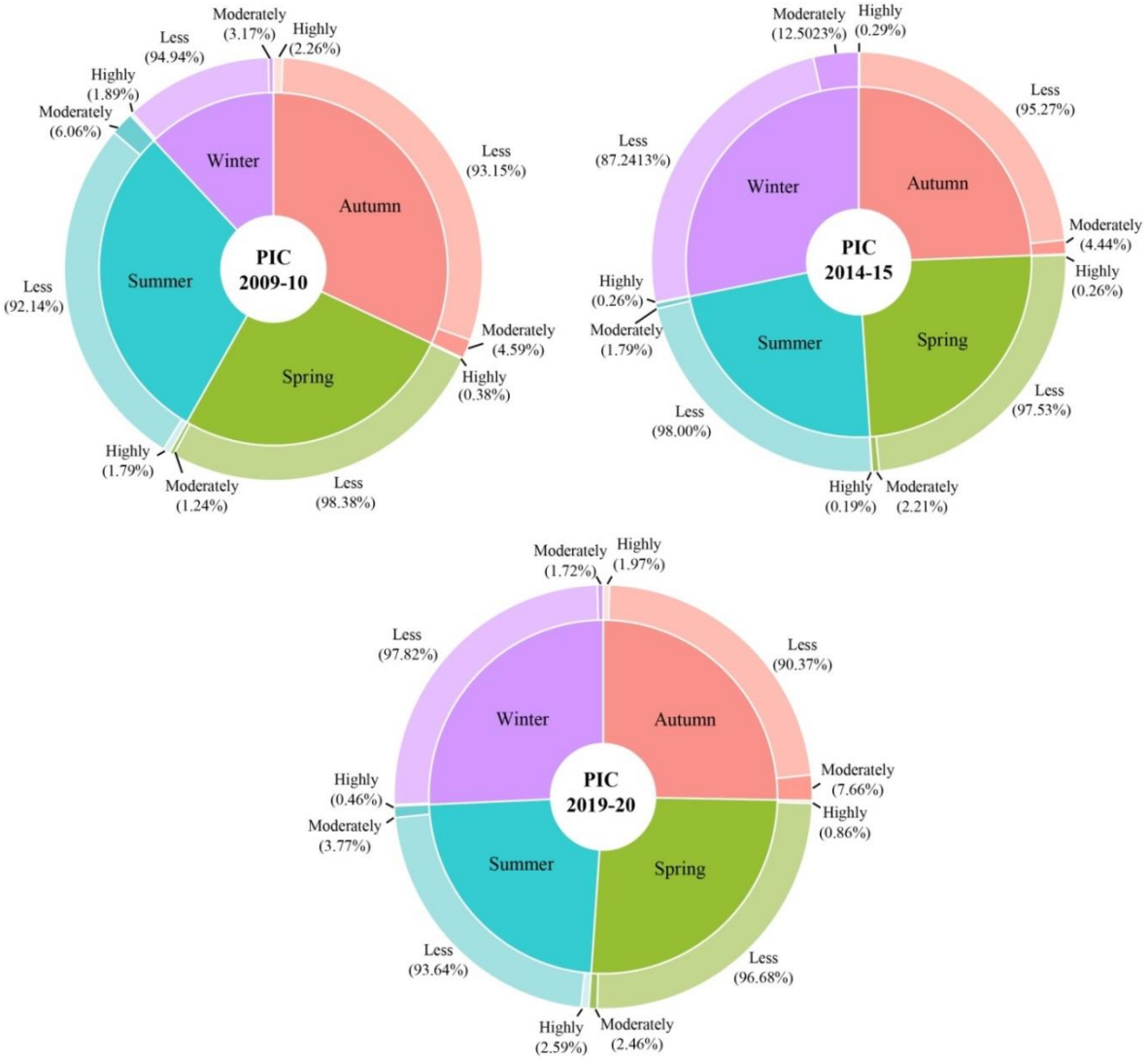

Fig. 10 *Percentage of yearly and seasonal productivity according to PIC concentration in the EEZ are of the Bay of Bengal over three years categorized as highly productive, moderately productive and less productive.*

4.1.4 Carbon sequestration trending:

In terms of seasonal variation it shows that chl-a in winter and post-monsoon is decreasing as the year progresses, in pre-monsoon chl-a increased in 2014-15 and gradually decreased in 2019-20, where it increases as the years goes on during summer. On the other hand, POC of winter and summer has increasing trend where spring and autumn has decreasing trend. Respectively, during winter, spring, and summer there's a rising trend in PIC. In contrast, autumn exhibit a declining trend. In this case, rising trends in winter and summer of POC and PIC indicates a rise in carbon sequestration activities.

In terms of annual variation, average maximum value of chl-a observed 29.13 mgm^{-3}, 13.61 mgm^{-3} and 30.89 mgm^{-3} in 2009-10, 2014-15 and 2019-20 respectively. That means chl-a has increasing trend. However, in contrast POC observed 994.99 mgm^{-3}, 622.65 mgm^{-3} and 787.95 mgm^{-3} according to 2009-10, 2014-15 and 2019-20. This indicates a rising tendency for whereas PIC identified 0.08 mgm^{-3}, 3.67 mgm^{-3}, and 0.09 mgm^{-3} respectively. This suggests that PIC is trending upward. PIC, POC and Chl-a are trending upward in this instance, which indicates an increase in carbon sequestration processes.

4.2. Seasonal variability 2018 (Winter vs. Monsoon)

4.2.1 Primary productivity

On the other hand, throughout the winter and monsoon seasons, there was also observed a noticeable surface-bottom and station-wise variation in chlorophyll-a. The stations with the highest concentration of total chlorophyll-a during the winter were Teknaf (approximately 1.12 µg/l), next lower than Teknaf was Patenga (approximately 0.46 µg/l), followed by Cox's Bazar (averagely 0.24 µg/l), which is lower than Patenga. Comparatively lower than the Cox's Bazar was found in the Bashbaria station (approximately 0.21 µg/l), and the Kutubdia station (approximately 0.16 µg/l) had the lowest quantity of Chlrophyll-a (Table 7). Then the maximum Chlorophyll-a (about 1.39 µg/l) was reported at the Teknaf station during the monsoon season. Approximately 0.69 µg/l was reported at the Patenga station. The stations with the lowest levels of Chl-a were Cox's Bazar (about 0.29 µg/l), Bashbaria (roughly 0.21 µg/l), and Kutubdia (approximately 0.06 µg/l) (Table 8). Although Chl-a is increasing uniformly at all of the stations over the two seasons, the monsoon season is when the maximum chlorophyll-a was seen. The season GIS modeling illustrates the spread of Chl-a in the northern BoB (Fig 11).

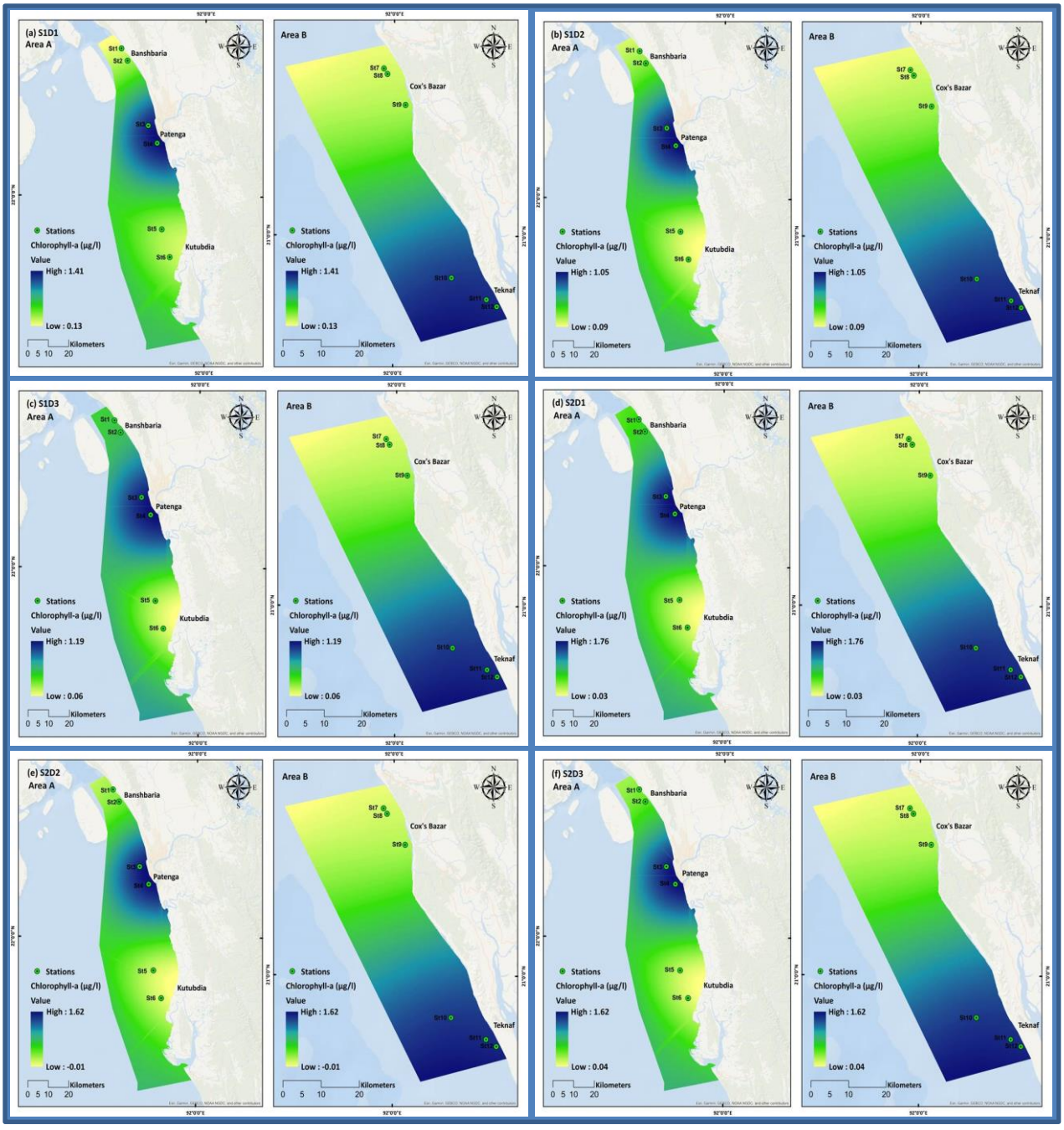

Fig. 11 (a-f) *Seasonal variation in Chlorophyll-a (µg/l) profile. The color difference indicating the seasonal variation between surface, middle and bottom Chlorophyll-a: S1=*

Winter, S2= Monsoon, D1= Surface (0 m), D2= Middle (5m), D3= Bottom (10 m). Here a) S1D1; b) S1D2; c) S1D3; d) S2D1; e) S2D2 and f) S2D3

Figure 12 informed us as stations 10,11 and 12 exhibit the highest Chl-a content at the surface, ranging from 1 to 1.3 µg/l. Stations 1-2 and 5-6 display low Chl-a content at the surface. In contrast, Stations 3-4 and 7-9 show a moderate level of Chl-a content, ranging from 0.27 to 0.58 µm/l. This pattern is generally maintained at a depth of 10 meters, with the exception of Stations 3 and 4.

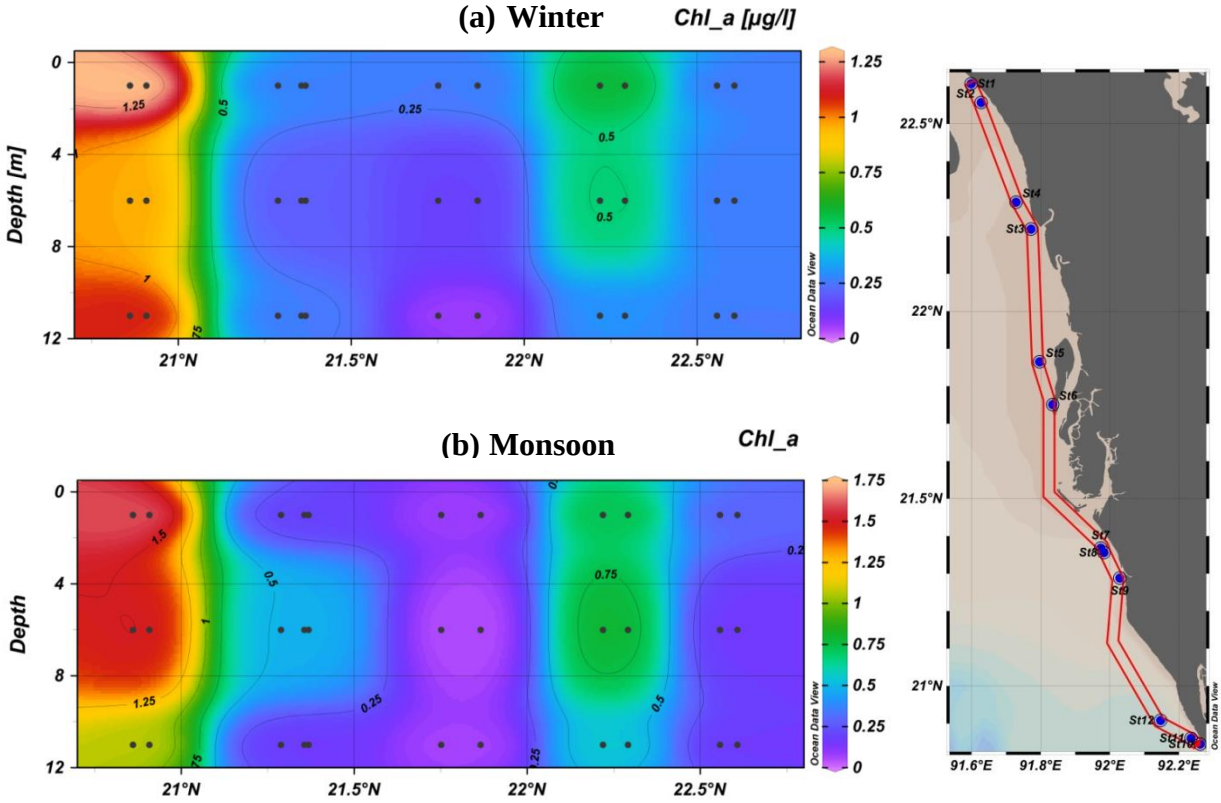

Fig. 12 *Depth variation in Chlorophyll-a (µg/l) profile during winter and monsoon season*

4.2.2 Carbon Flux concentration

At Northern BoB, the dominant seasonal patterns (winter and monsoons) largely determine the structure of the surface, middle, and bottom Carbon Flux. In particular, surface to bottom station wise variation in carbon flux during winter season was identified as the highest amount in the Teknaf station (approximately 14.16 mg C m^{-2} day^{-1}), approximately 7.77 mg C m^{-2} day^{-1} found in the Patenga station which is lower than Teknaf station, then averagely 3.68 mg C m^{-2} day^{-1} was found in Bashbaria station which is lower compare to Patenga station, comparatively lower than the Bashbaria was found in the Kutubdia station (approximately 2.12 mg C m^{-2} day^{-1}) and the lowest amount was found in the Cox's Bazar station (approximately 1.15 mg C m^{-2} day^{-1}) . In the monsoon season the highest amount of carbon flux was also found in the Teknaf station (approximately 6.89 mg C m^{-2} day^{-1}), comparatively lower amount was found in the Patenga station (approximately 8.24 mg C m^{-2} day^{-1}), then lower than that was found in the Bashbaria station (approximately 5.59 mg C m^{-2} day^{-1}) then in cox's Bazar (approximately 2.35 mg C m^{-2} day^{-1}) and the lowest amount was found in the Kutubdia station (approximately 1.41 mg C m^{-2} day^{-1}). Here carbon flux is increasing equally in all the stations of two seasons, but the highest carbon flux was found during monsoon season. The distribution of CF in the northern BoB is shown by the season GIS modeling (Fig 13).

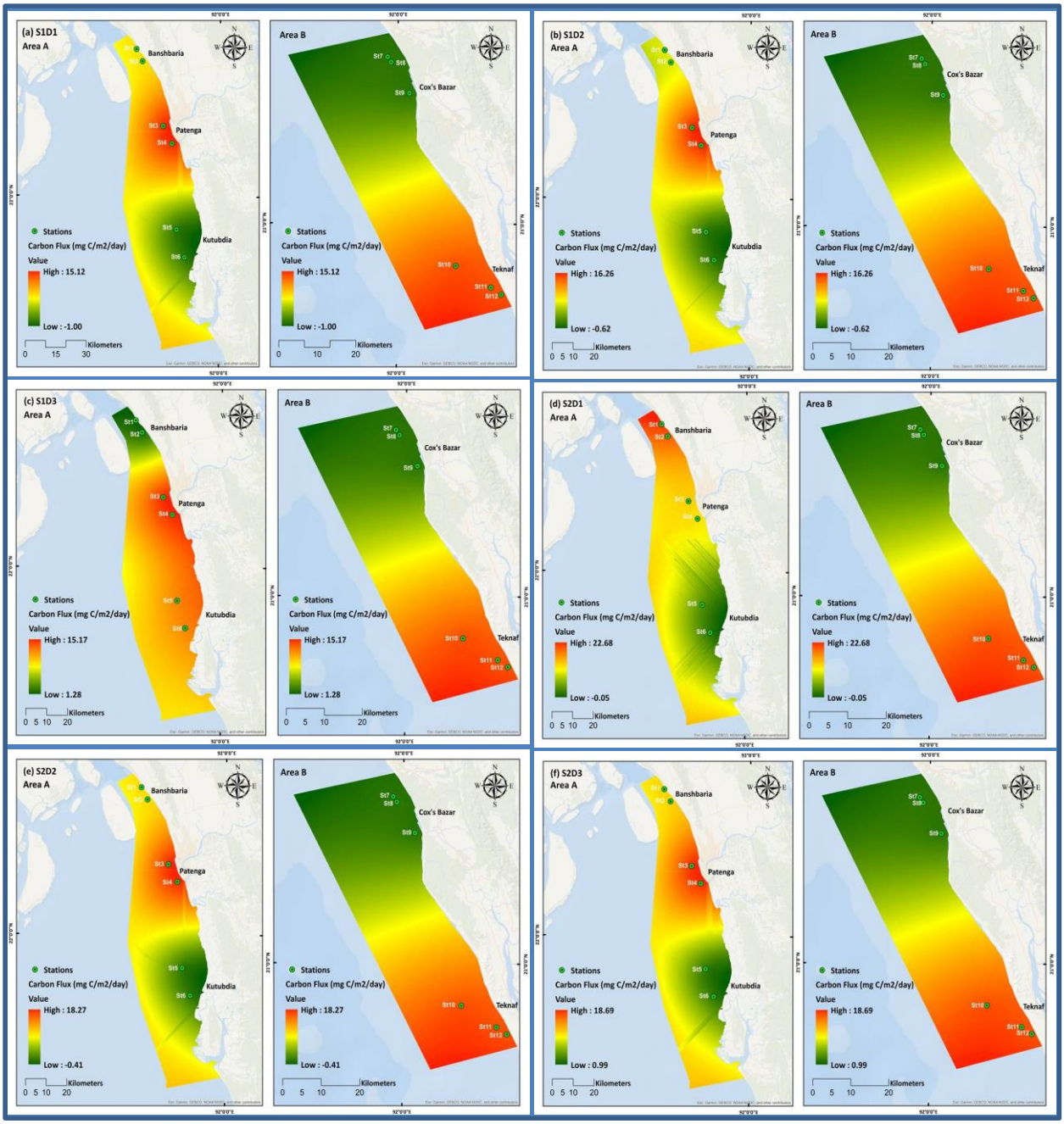

Fig. 13 (a-f) *Seasonal variation in Carbon Flux (mg C m^{-2} day^{-1}) profile. The color difference indicating the seasonal variation between surface, middle and bottom carbon flux: S1= Winter, S2= Monsoon, D1= Surface (0 m), D2= Middle (5m), D3= Bottom (10 m). Here a) S1D1; b) S1D2; c) S1D3; d) S2D1; e) S2D2 and f) S2D3*

As depicted in Figure 14, stations 10, 11, and 12 had surface CF content that was significantly elevated, ranging from 12 to 13.74 mg C m^{-2} day^{-1}. The moderate CF range of 7.5 to 7.69 mg C m^{-2} day^{-1} was observed at stations 3-4. In contrast, the surface CF levels at stations 1-2 and 5-9 were significantly lower. Overall this trend held true down to a depth of 10 meters.

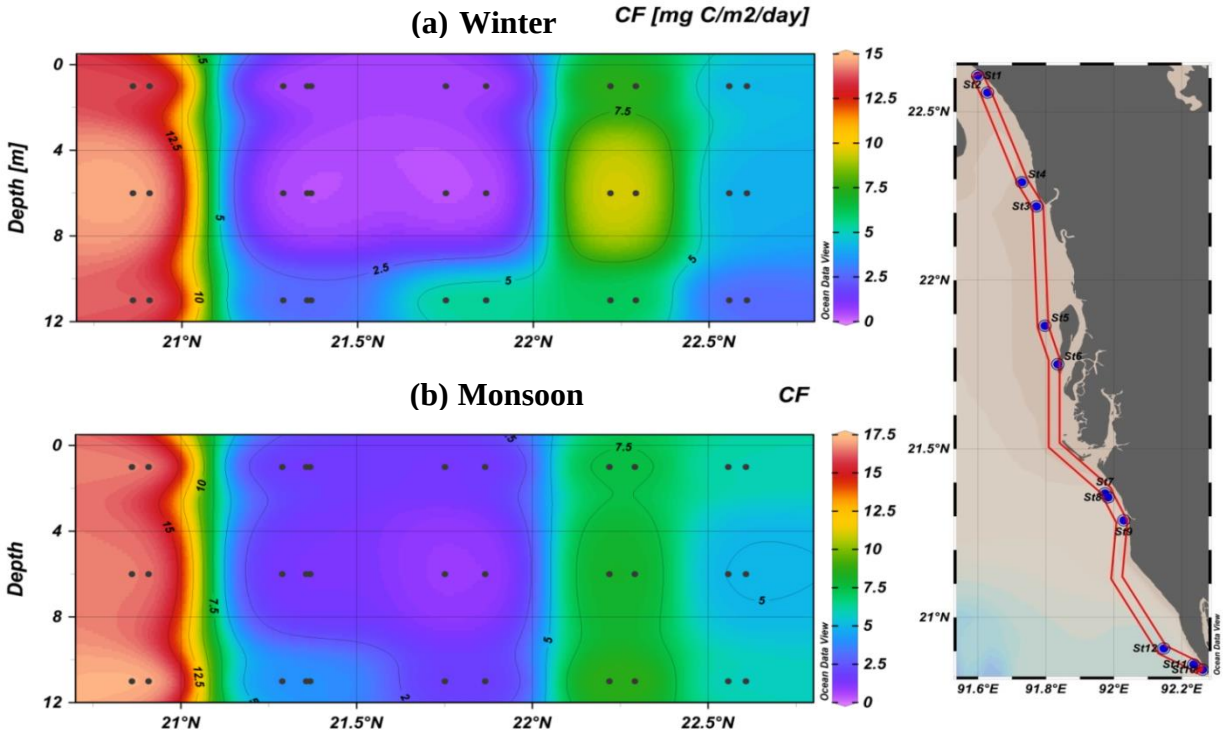

Fig. 14 *Depth variation in Carbon Flux (mg C m^{-2} day^{-1}) profile during winter and monsoon season*

\

4.2.3 Total Carbon content

In contrast, a notable surface-bottom and station-wise variation in Total Carbon observed during winter and monsoon season. The stations with the highest concentration of TC during the winter were Teknaf (approximately 5.64 mgm^{-3}), then Kutubdia (approximately 4.16 mgm^{-3}) which is lower than Teknaf, next Patenga (averagely 3.04 mgm^{-3}), which is lower than Kutubdia, comparatively lower than the Patenga was found in the Cox's Bazar station (approximately 2.89 mgm^{-3}), and the Bashbaria station (approximately 1.95 mgm^{-3}) had the lowest quantity of TC (Table 11). During the monsoon season, the Teknaf station recorded the highest total carbon (approximately 7.74 mgm^{-3}). The Cox's Bazar station recorded a relatively lower amount (approximately 5.62 mgm^{-3}), next the Kutubdia station (approximately 4.82 mgm^{-3}), then Patenga station (approximately 3.58 mgm^{-3}), and the Bashbaria station (approximately 2.13 mgm^{-3}) had the lowest quantity of TC (Table 12). Here, the carbon flux is not rising uniformly at all stations during the two seasons; nonetheless, the monsoon season yielded the largest carbon flux. The season GIS modeling illustrates the spread of CF in the northern BoB (Fig 15).

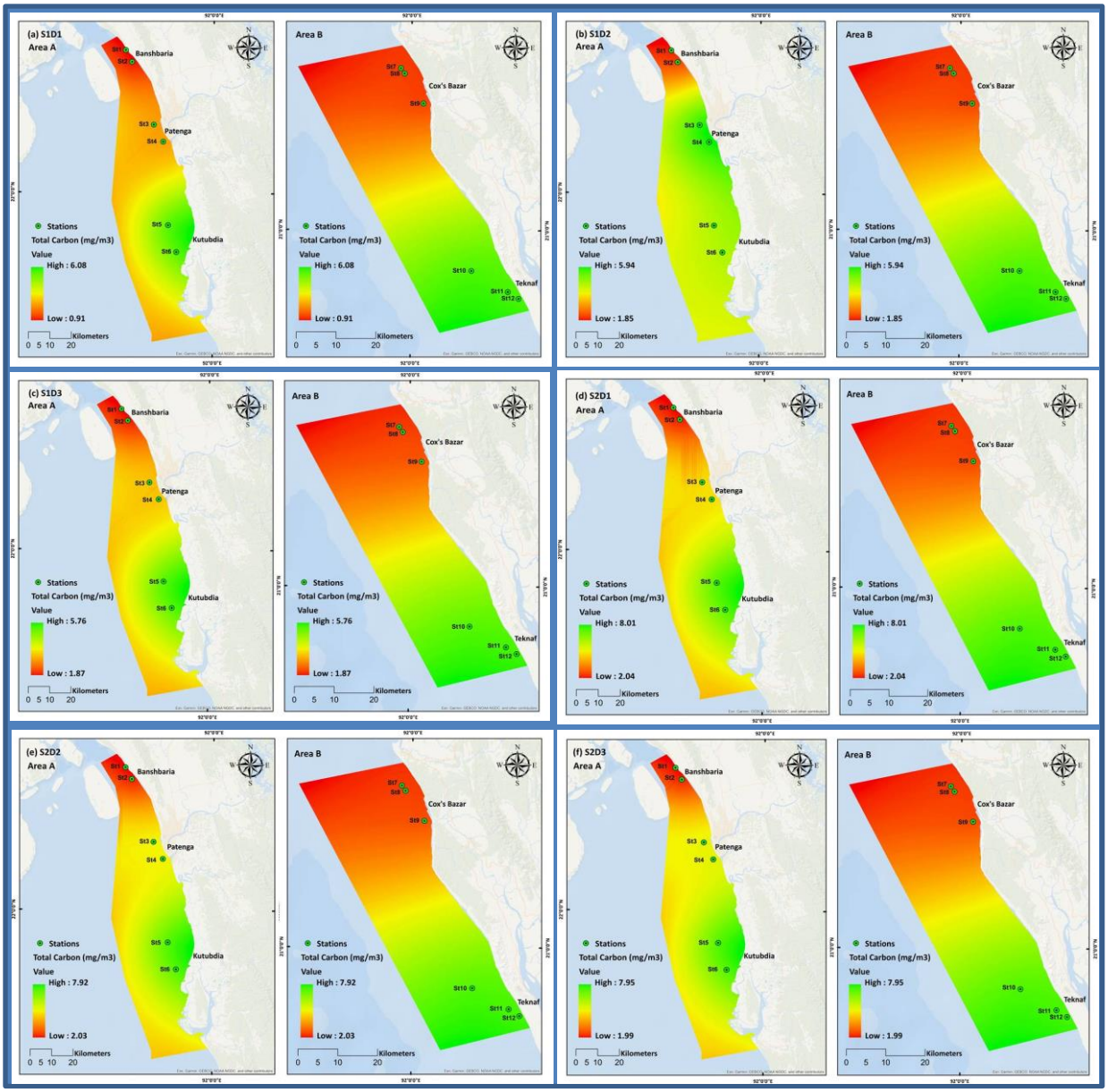

Fig. 15 (a-f) *Seasonal variation in Total Carbon (mgm^{-3}) profile. The color difference indicating the seasonal variation between surface, middle and bottom total carbon: S1= Winter, S2= Monsoon, D1= Surface (0 m), D2= Middle (5m), D3= Bottom (10 m). Here a) S1D1; b) S1D2; c) S1D3; d) S2D1; e) S2D2 and f) S2D3*

According to Figure 16, the stations 10, 11, and 12 had the greatest amounts of TC content at the surface, ranging from 5.64 to 7.74 mgm^{-3}. Conversely, stations 1-2 and 7-9 showed lower amounts of TC at the surface ranging from 1.62 to 3.9 mgm^{-3}. In the meantime, the TC levels at stations 3–6 were moderate. Stations 7-9 somewhat varied from this observed distribution, but overall it was constant down to 10 meters.

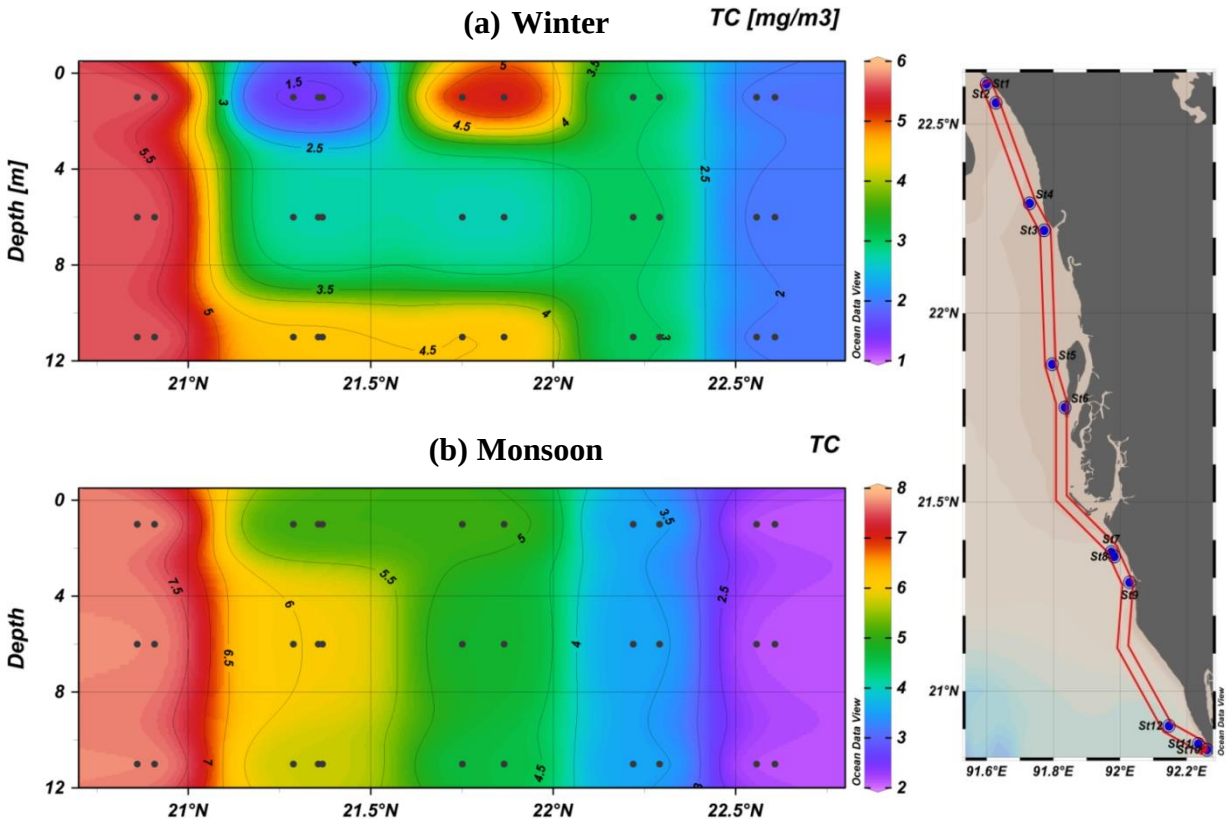

Fig. 16 *Depth variation in Total Carbon (mgm^{-3}) profile during winter and monsoon season*

4.2.4 Sinking rate of plankton

Specifically, the variation in Phytoplankton sinking rate from surface to bottom station wise during the winter season was found to be as follows: the highest amount was found in the Patenga station (approximately 2.56 $mday^{-1}$), followed by the Teknaf station (approximately 2.51 $mday^{-1}$); Bashbaria station (average 1.89 $mday^{-1}$) and Kutubdia station (about 0.48 $mday^{-1}$). During the monsoon, the Bashbaria station recorded the highest PSR (approximately 2.63 m/da $mday^{-1}$). The Patenga station recorded a relatively lower amount (approximately 2.3 $mday^{-1}$), followed by the Teknaf station (approximately 2.22 $mday^{-1}$), Cox's Bazar (approximately 0.42 $mday^{-1}$), and Kutubdia station (approximately 0.29 $mday^{-1}$) Even though the phytoplankton sinking rate in this case is not increasing consistently at all stations throughout the course of the two seasons, the monsoon season produced the highest phytoplankton sinking rate. The expansion of PSR in the northern BoB is depicted by the season GIS modeling (Fig 17).

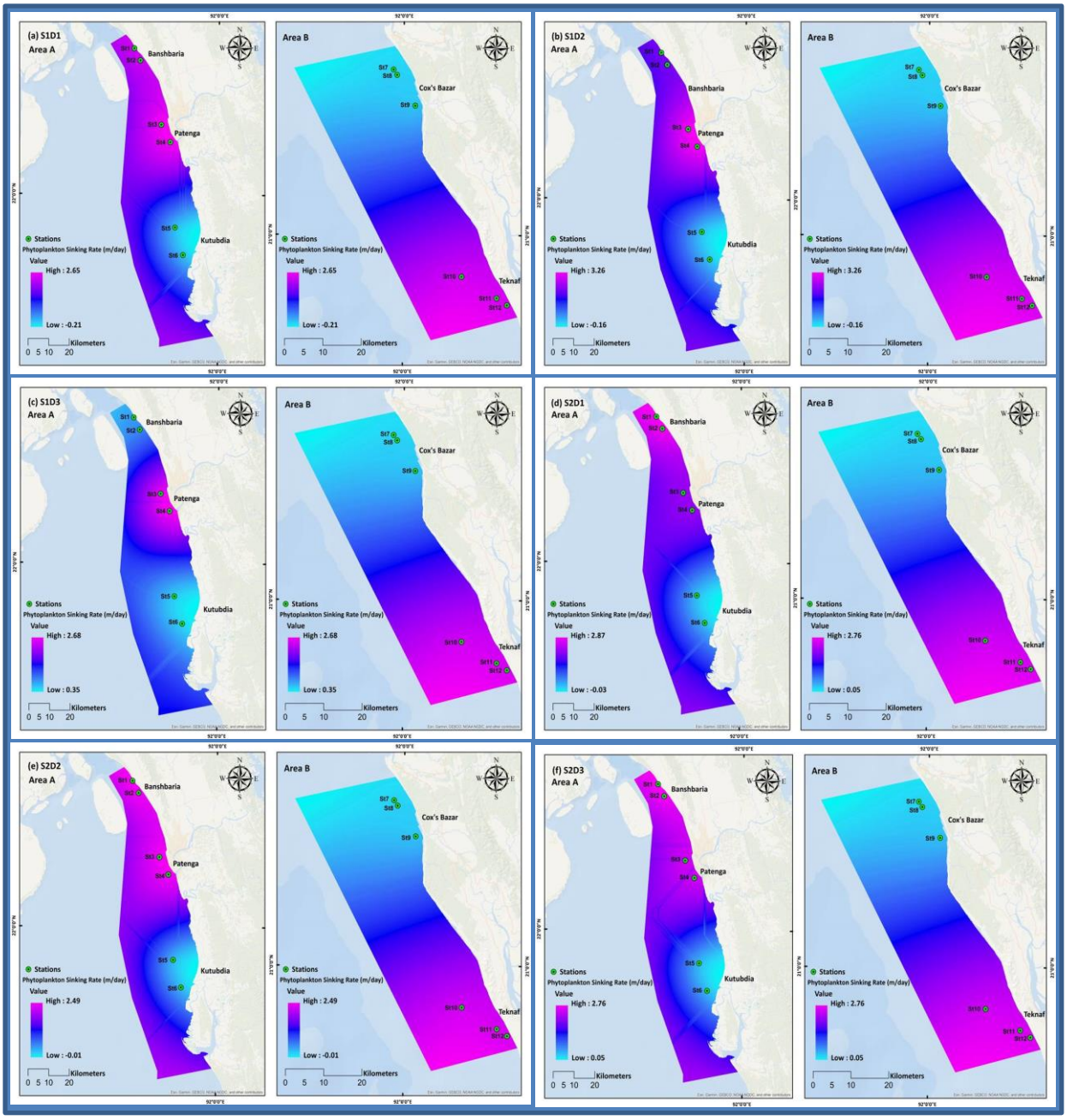

Fig. 17 (a-f) *Seasonal variation in Phytoplankton sinking rate (mday^{-1}) profile. The color difference indicating the seasonal variation between surface, middle and bottom Phytoplankton sinking rate: S1= Winter, S2= Monsoon, D1= Surface (0 m), D2= Middle (5m), D3= Bottom (10 m). Here, a) S1D1; b) S1D2; c) S1D3; d) S2D1; e) S2D2 and f) S2D3*

Here, stations 1-4 and 10-12 had the greatest surface concentrations of ranging from 2 to 2.39 mday^{-1}, according to Figure 18. By comparison, stations 5-9 showed lower levels of ranging from 0.3 to 0.32 mday^{-1}. Up to a depth of ten meters, the general tendency held true, despite stations 1-2 departing somewhat from the observed pattern.

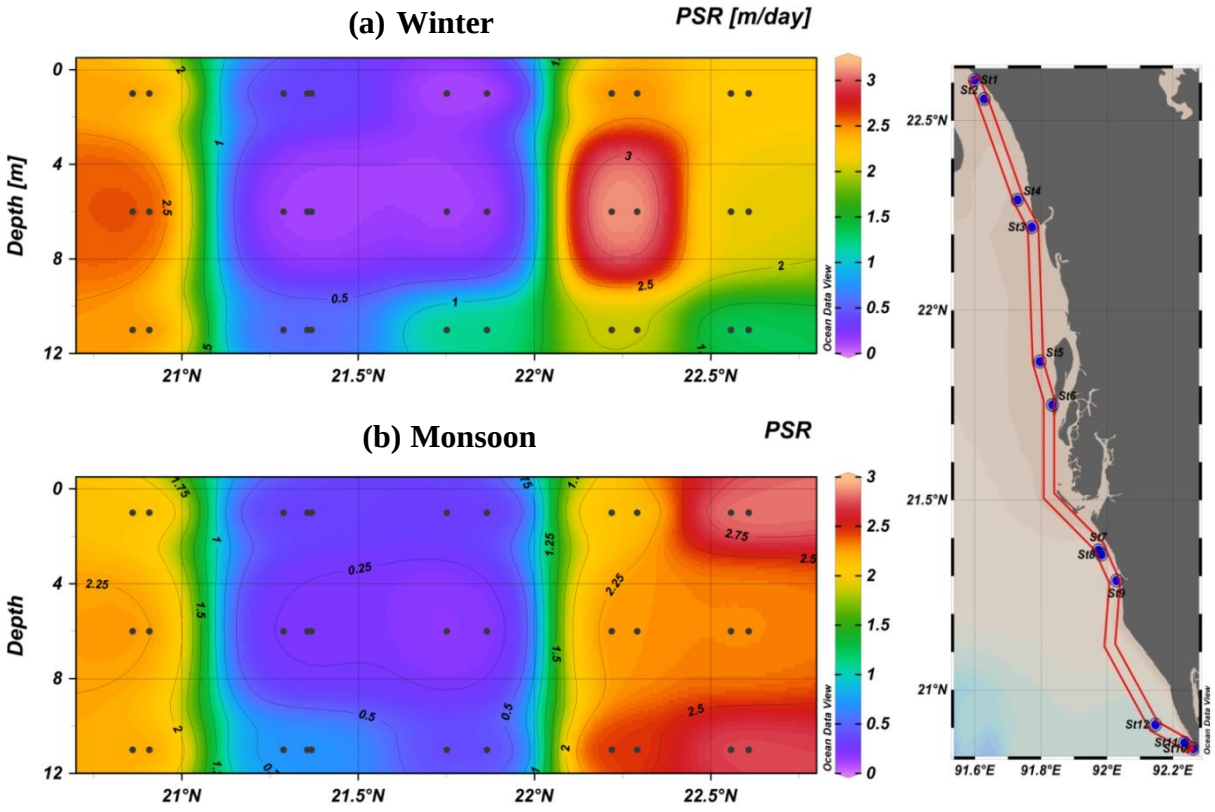

Fig. 18 *Depth variation in Phytoplankton Sinking Rate (mday^{-1}) profile during winter and monsoon season*

4.2.5 Carbon sequestration trending in two seasons

Average chlorophyll-a 0.44 µg/l and 0.53 µg/l was observed in winter and monsoon, whereas approximately 5.78 mg C m^{-2} day^{-1} and 6.89 mg C m^{-2} day^{-1} CF; 3.54 mgm^{-3} and 4.78 mgm^{-3} TC; 1.56 $mday^{-1}$ and 1.57 $mday^{-1}$ PSR was identified during winter and monsoon. The increasing patterns seen in the monsoon of chl-a, TC and PSR in this instance suggest an increase in carbon sequestration efforts.

In terms of depth variation, average CF of winter and monsoon observed in surface about 6.39 mg C m^{-2} day^{-1}, in middle 6.48 mg C m^{-2} day^{-1} and in bottom 7.29 mg C m^{-2} day^{-1}. Whereas the average TC was identified 4.24 mgm^{-3} at the surface, 4.28 mgm^{-3} in the middle, and 4.61 mgm^{-3} in the bottom. Maximum PSR (1.6 $mday^{-1}$) observed at deep water, relatively lower PSR (1.51 $mday^{-1}$) found at middle and in the surface (1.51 $mday^{-1}$). This suggests that as depth increases, phytoplankton's sinking rate , carbon flux and total carbon increase.

4.3 Seasonal variability 2020 (Four seasons)

4.3.1 Primary productivity level

More specifically, it was identified during the winter. There was the following difference in Chl-a from surface to bottom station wise. Cox's bazar shows the highest chl-a (0.22 µg/l) than Kutubdia. During Pre-monsoon Cox's Bazar also identified as the most Chl-a (0.41). Followed by Monsoon and Post-monsoon also shows the Cox's bazar as highest Chl-a than Kutubdia (Fig 19).

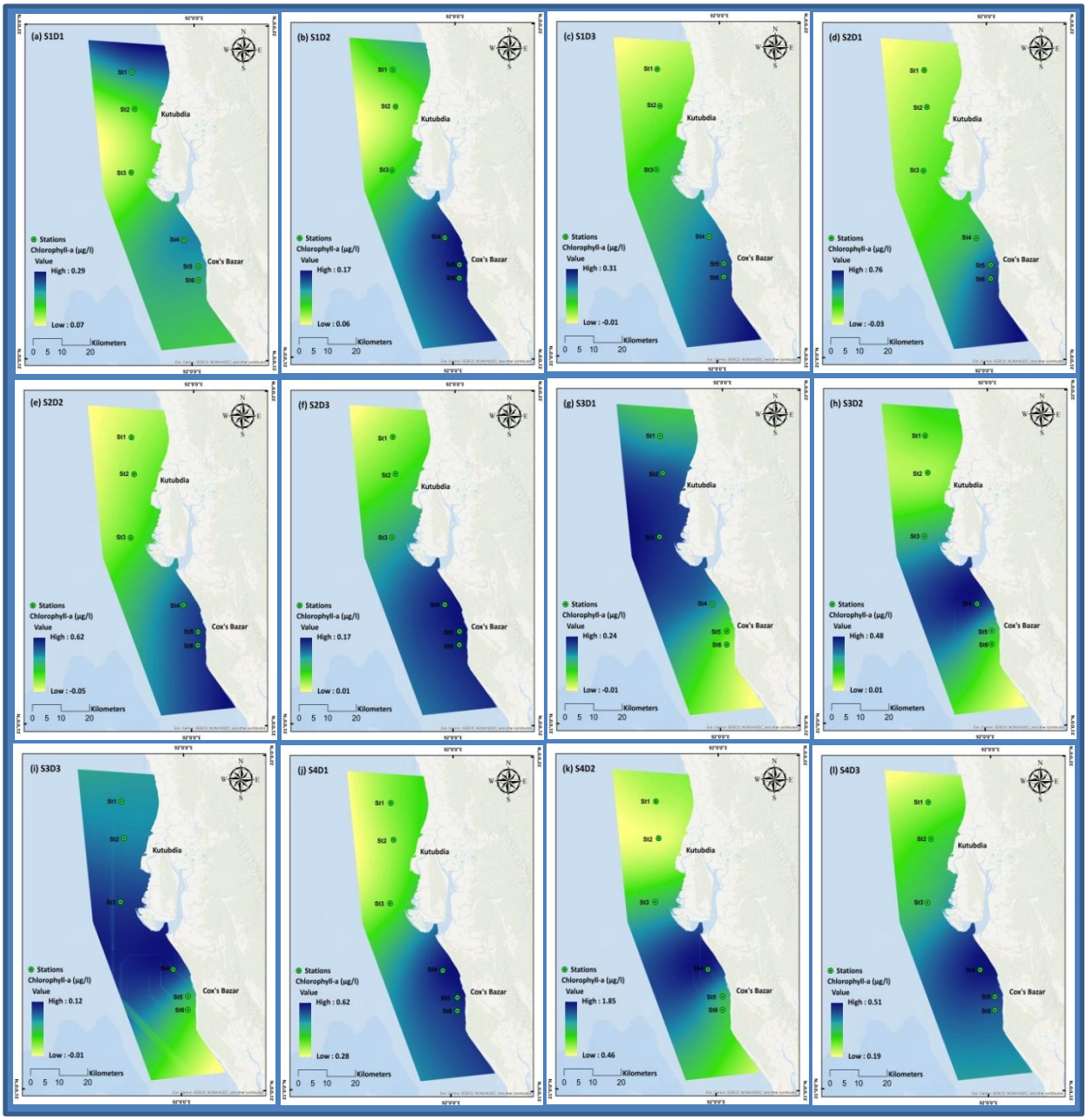

Fig. 19 (a-l) *Seasonal variation in Chlorophyll-a (µg/l) profile. The color difference indicating the seasonal variation between surface, middle and bottom Chlorophyll-a: S1= Winter, S2= Pre-monsoon, S3=Monsoon, S4=Post-monsoon, D1= Surface (0 m), D2= Middle (5m), D3= Bottom (10 m). Here, a) S1D1; b) S1D2; c) S1D3; d) S2D1; e) S2D2; f) S2D3 g)S3D1; h)S3D2;ij)S3D3; j)S4D1; k) S4D2 and l) S4D3*

Based on Figure 20, the stations with the highest surface concentrations of Chl-a were 1 and 4-6, with values 0.18-0.2 µg/l. In contrast, stations 2-3 displayed lower Chl-a concentrations,

ranging from 0.07 to 0.1 µg/l. The overall tendency persisted up to a depth of 10 meters, however station 1 slightly deviated from the pattern that was seen. This pattern also seen in the pre-monsoon except the depth of 10m (Station 4-6) and surface (Station 1). On the other hand, during monsoon and post-monsoon the highest chl-a observed in middle ocean, where station 4-6 show high concentration and station 1-3 show lower concentration but in surface and deep ocean every stations show lower concentration.

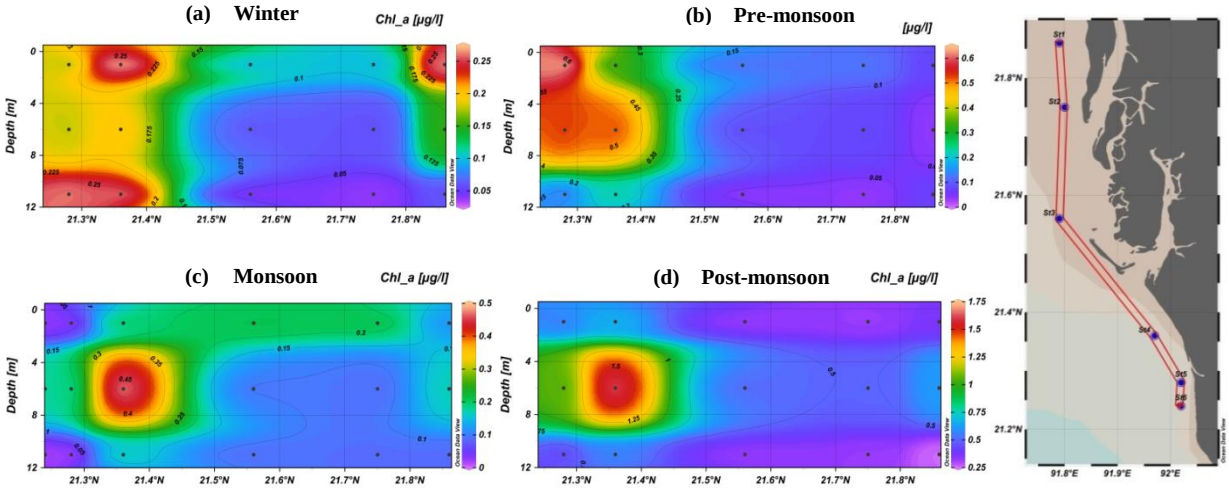

Fig. 20 *Depth variation in Chlorophyll-a (µg/l) profile during four seasons*

4.3.2 Carbon Flux concentration

The following was the variation in CF station-wise between the surface and bottom. The highest CF (2.42 mg C m^{-2} day^{-1}) is observed in Cox's bazaar during winter. Followed by Kutubdia is with higher CF (2.65 mg C m^{-2} day^{-1}) in pre-monsoon, Cox's Bazar (2.41 mg C m^{-2} day^{-1}) in monsoon and Kutubdia (2 mg C m^{-2} day^{-1}) in post-monsoon (Fig 21).

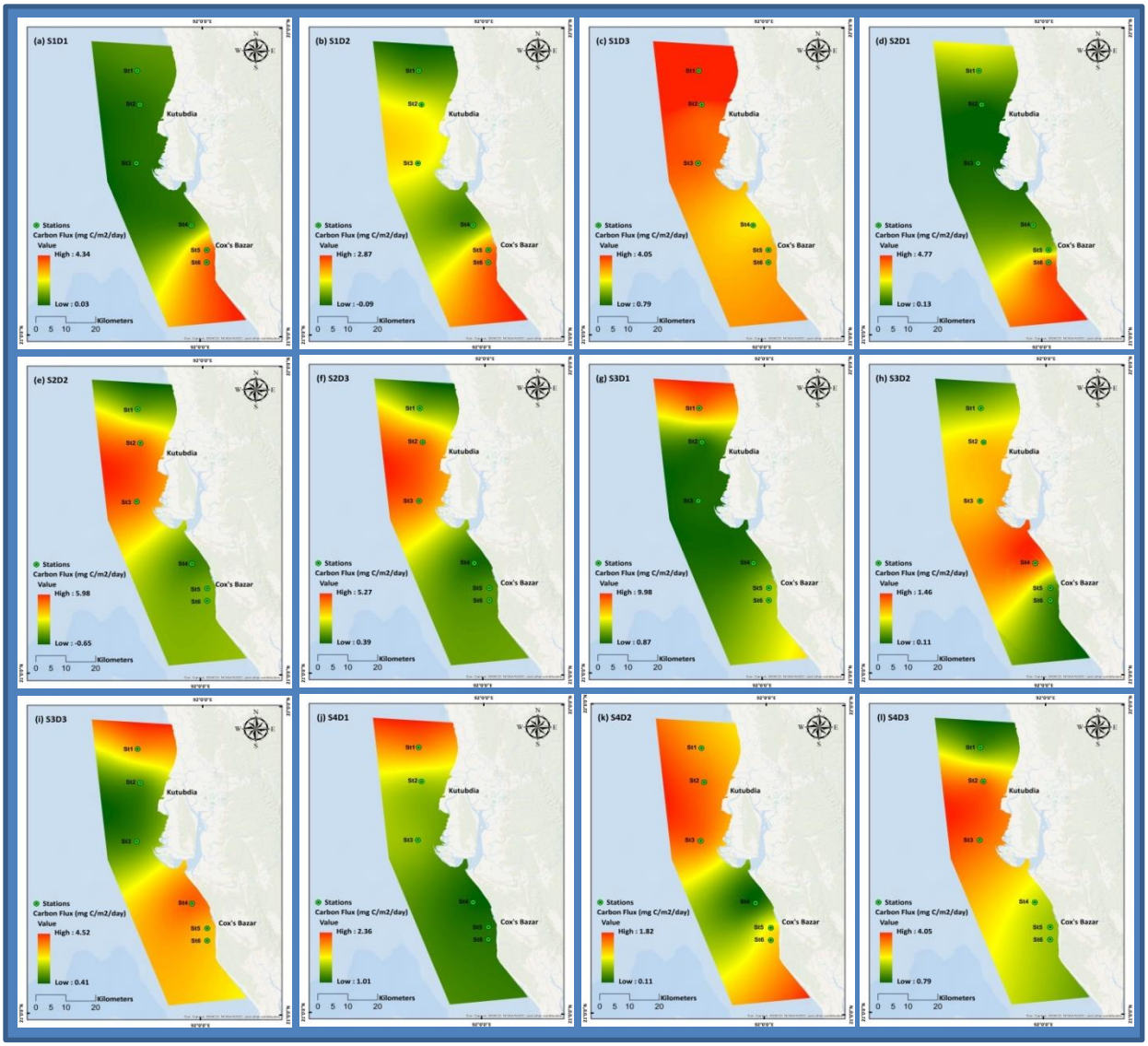

Fig. 21 (a-l) *Seasonal variation in Carbon Flux (mg C m^{-2} day^{-1}) profile. The color difference indicating the seasonal variation between surface, middle and bottom Carbon Flux: S1= Winter, S2= Pre-monsoon, S3=Monsoon, S4=Post-monsoon, D1= Surface (0 m), D2= Middle (5m), D3= Bottom (10 m). Here, a) S1D1; b) S1D2; c) S1D3; d) S2D1; e) S2D2; f) S2D3 g)S3D1; h)S3D2;ij)S3D3; j)S4D1; k) S4D2 and l) S4D*

With values ranging from 4.35-5 mg C m^{-2} day^{-1}, stations 1-3 had the greatest deep water concentrations of according to Figure 22. On the other hand, stations 4-6 showed moderate levels of ranging from 2.91 to 3.5 mg C m^{-2} day^{-1} where station 1-5 show lower CF content except station 6 in surface during winter. The pre-monsoon also exhibits this pattern in 10m

depth except station 1 and 4-6 where in the surface al stations are identified with lower CF content. This pattern is also identified in the post-monsoon.

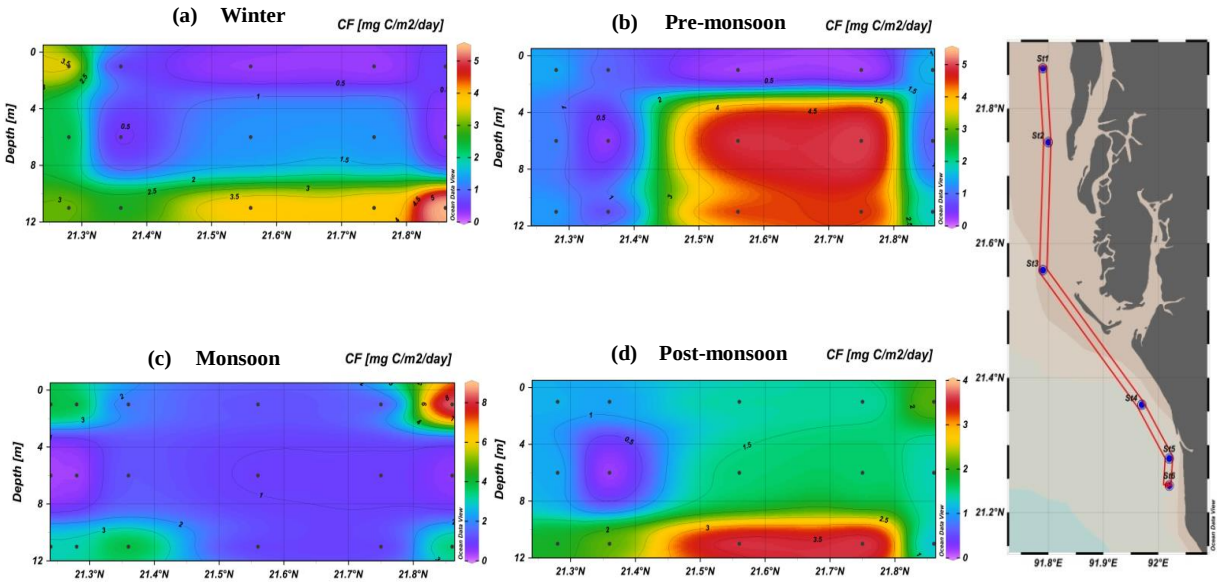

Fig. 22 *Depth variation in Carbon Flux mg C m^{-2} day^{-1}) profile during four seasons*

4.3.3 Total Carbon content

In Cox's Bazaar, the highest TC (4.55 mgm^{-3}) was observed during winter and Kutubdia had the highest TC (6.85 mgm^{-3}) during the pre-monsoon period while Kutubdia had the highest TC (5.47 mgm^{-3}) during the monsoon. Furthermore, in the post-monsoon season, Cox's Bazar observed most TC of 4.75 mgm^{-3}) (Fig. 33).

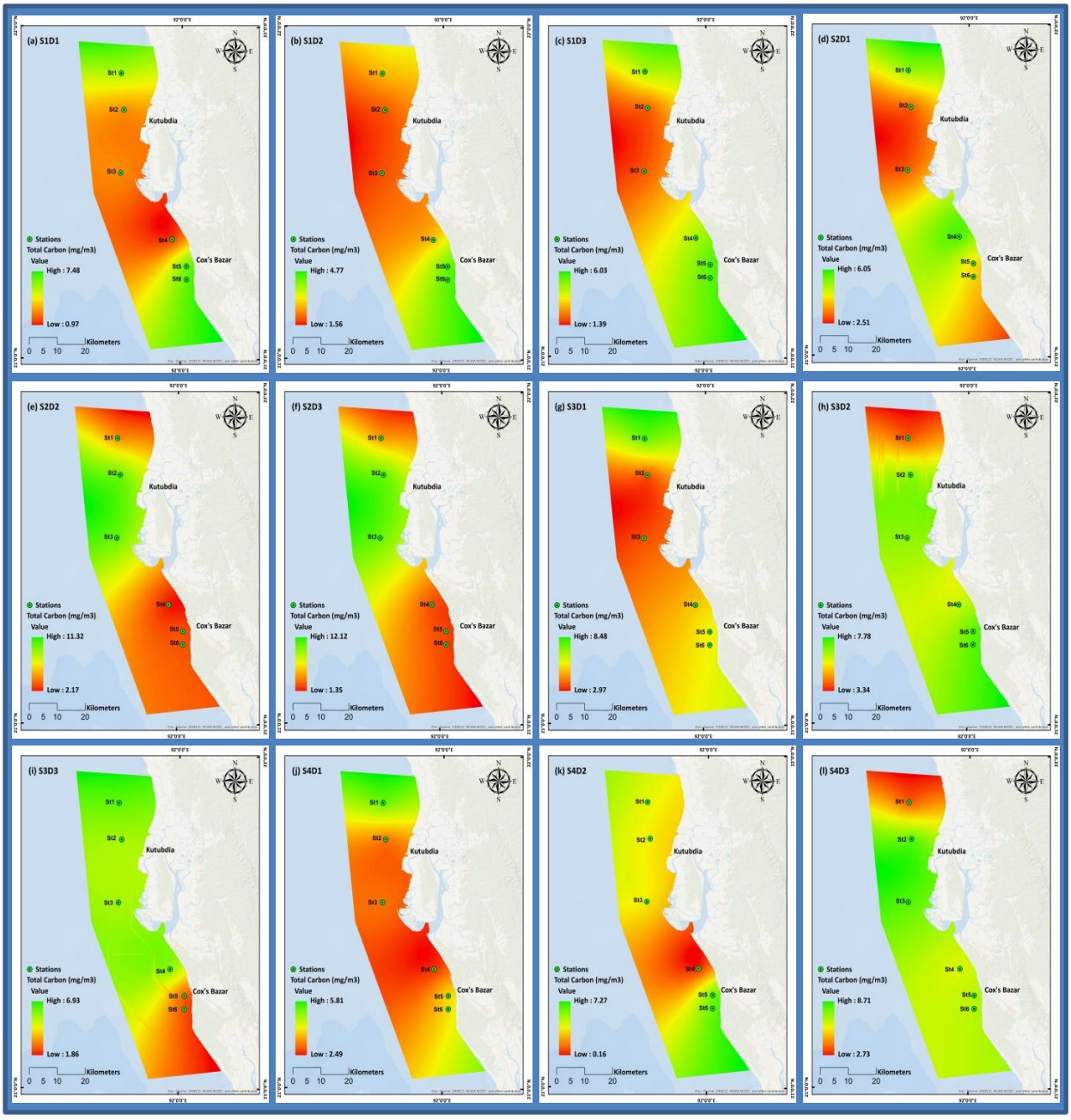

Fig. 23 (a-l) *Seasonal variation in Total Carbon (mgm^{-3}) profile. The color difference indicating the seasonal variation between surface, middle and bottom Total Carbon: S1= Winter, S2= Pre-monsoon, S3=Monsoon, S4=Post-monsoon, D1= Surface (0 m), D2= Middle (5m), D3= Bottom (10 m). Here, a) S1D1; b) S1D2; c) S1D3; d) S2D1; e) S2D2; f) S2D3 g)S3D1; h)S3D2;ij)S3D3; j)S4D1; k) S4D2 and l) S4D3*

The highest deep water concentrations of TC were found in stations 2-3, with values ranging from 8-10.62 mgm^{-3}. By contrast, station 1 and 4-6 displayed lower levels of TC content, ranging from 2-3.11 mgm^{-3} where surface water displayed down TC content during pre-monsoon and post-monsoon. In contrast to, during monsoon maximum TC found in the middle than surface and deep where low amount of TC observed in the surface to bottom in all stations except station 1 and 3 (Fig. 24).

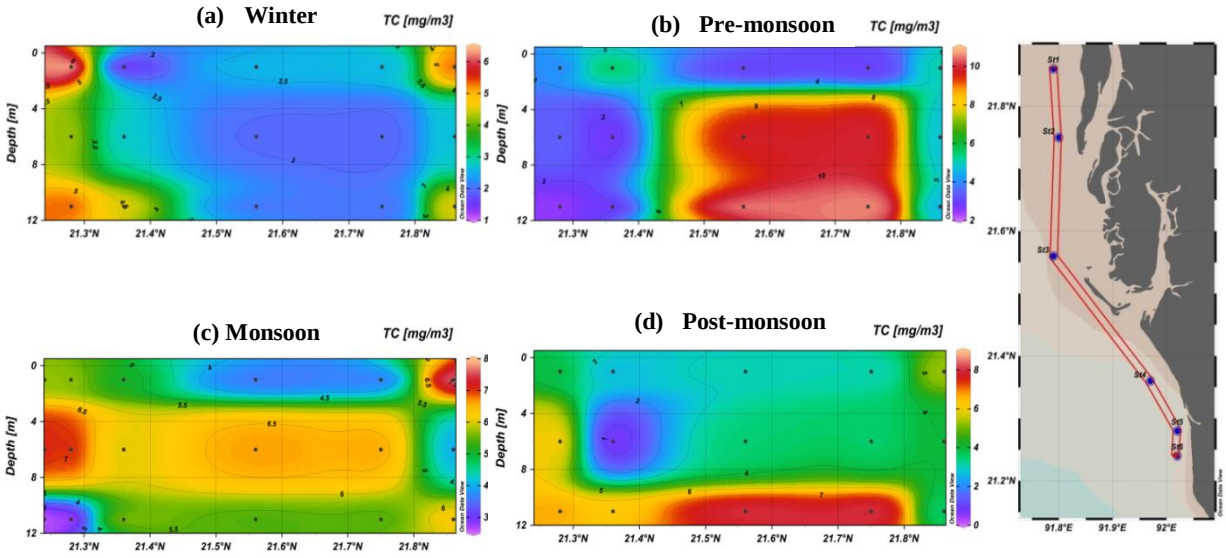

Fig. 24 *Depth variation in TC (mgm^{-3}) profile during four seasons*

4.3.4 Sinking rate of plankton

The maximum PSR concentration was 0.74 ($mday^{-1}$) in Kutubdia throughout the winter. Conversely, during the pre-monsoon and monsoon periods, respectively, Cox's Bazar attained its peak PSR levels of 0.33 ($mday^{-1}$) and 0.57 ($mday^{-1}$), respectively. During the post-monsoon season, 0.42 ($mday^{-1}$) of PSR was reported by Kutubdia (Fig. 25).

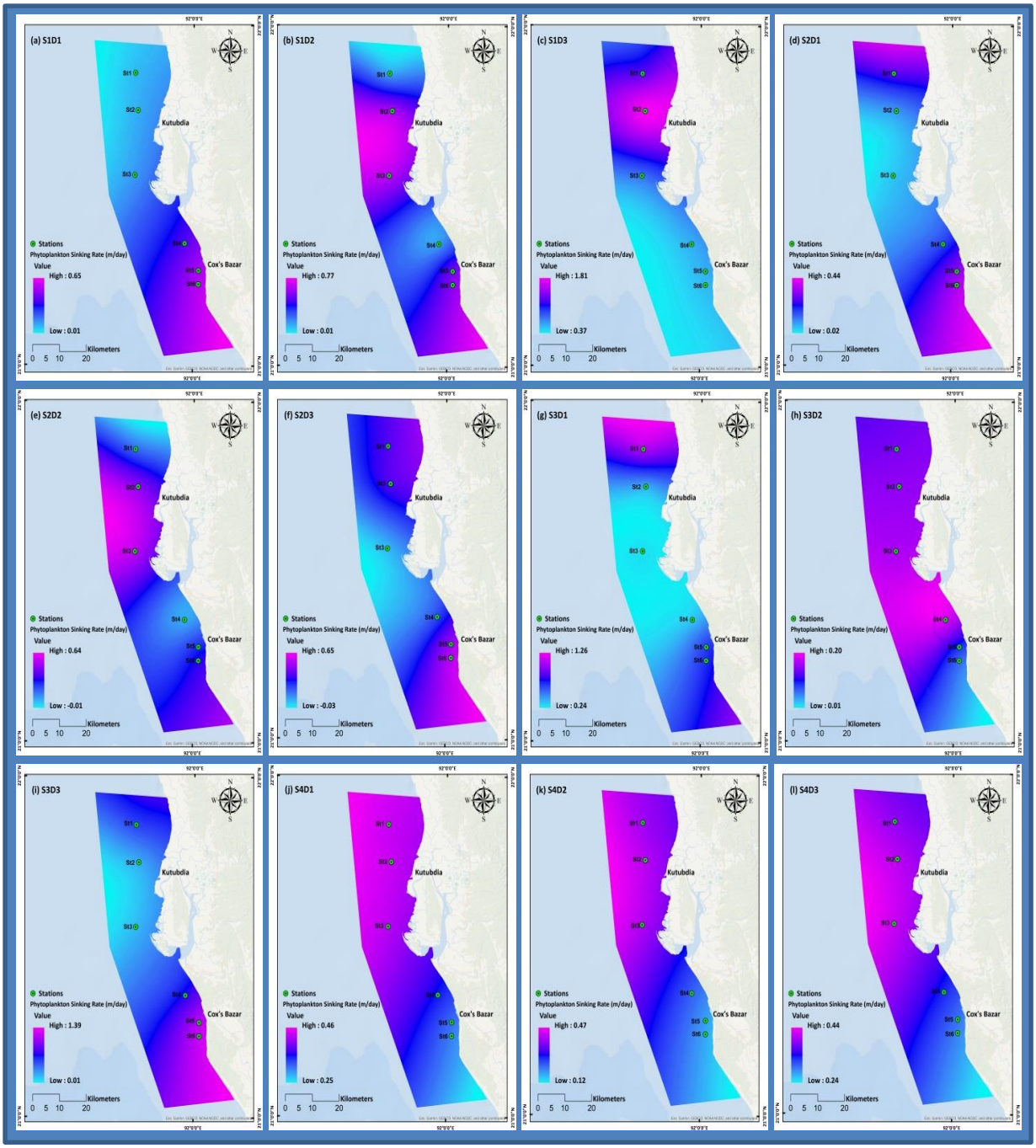

Fig. 25 (a-l) *Seasonal variation in Plankton Sinking Rate (mday^{-1}) profile. The color difference indicating the seasonal variation between surface, middle and bottom Plankton Sinking Rate: S1= Winter, S2= Pre-monsoon, S3=Monsoon, S4=Post-monsoon, D1= Surface (0 m), D2= Middle (5m), D3= Bottom (10 m). Here, a) S1D1; b) S1D2; c) S1D3; d) S2D1; e) S2D2; f) S2D3 g)S3D1; h)S3D2;ij)S3D3; j)S4D1; k) S4D2 and l) S4D3*

Here maximum PSR content found during pre-monsoon and post monsoon. In the post-monsoon, higher PSR content displayed from surface to bottom in every station with ranging from 0.35 to 0.58 $mday^{-1}$ where pre-monsoon also followed same pattern except the surface water. On the other hand maximum PSR found in the 10m depth of water of the station 1-3, ranging from 1-1.64 $mday^{-}1$, where in the surface found low content in every station. During monsoon, the highest surface concentration observed in the station 1 (Fig. 26)

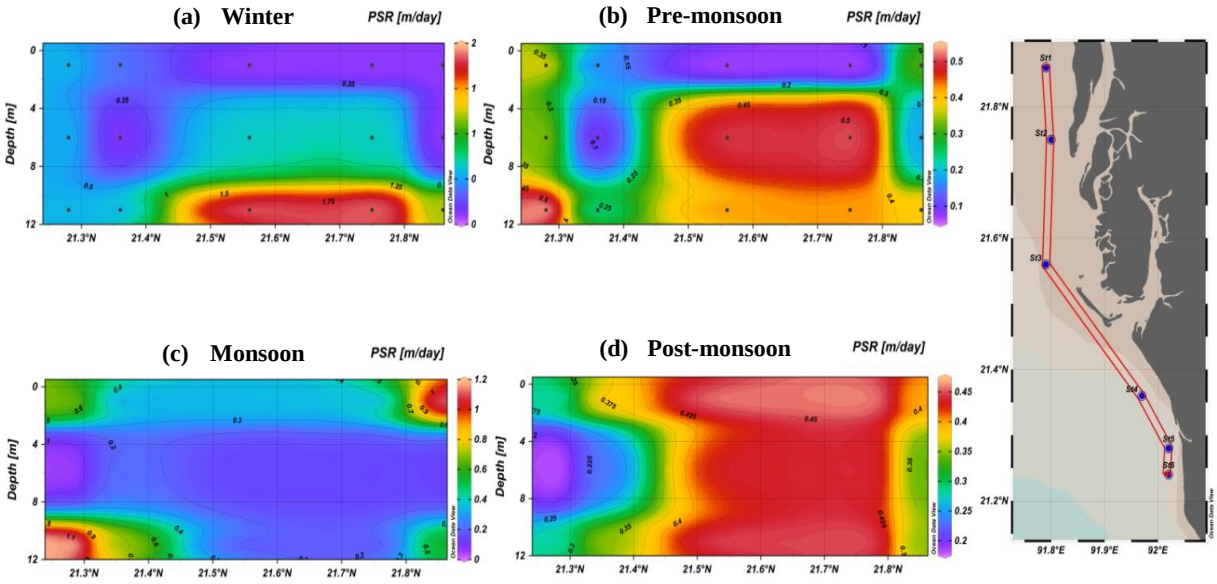

Fig. 26 *Depth variation in PSR ($mday^{-1}$) profile during four seasons*

4.3.5 Carbon sequestration trending in four seasons

Winter, pre-monsoon, monsoon and post-monsoon were associated with average levels of chl-a of 0.16 µg/l, 0.25 µg/l, 0.14 µg/l, 0.59 µg/l respectively; followed by 2.16 mg C m^{-2} day^{-1}, 1.87 mg C m^{-2} day^{-1}, 2.27 mg C m^{-2} day^{-1}, 1.64 mg C m^{-2} day^{-1} CF and 3.71 mgm^{-3}, 5.15 mgm^{-3}, 5.39 mgm^{-3}, 4.73 mgm^{-3} TC was observed. Where 0.62 $mday^{-1}$, 0.33 $mday^{-1}$, 0.46 $mday^{-1}$and 0.35 $mday^{-1}$ PSR was identified. In this case, the increasing patterns of chl-a, and PSR during the monsoon point to increased efforts at sequestering carbon.

The average CF for the winter, pre-monsoon, monsoon and post-monsoon was found to be 1.82 mg C m^{-2} day^{-1} at the surface, 1.36 mg C m^{-2} day^{-1} in the middle, and 2.76 mg C m^{-2} day^{-1} at the bottom, with respect to depth variation. Followed by TC values were found to be 3.63 mgm^{-3} at the top, 4.32 mgm^{-3} in the middle, and 5.13 mgm^{-3} in the bottom. Whereas deep water was the site of the most PSR (0.64 $mday^{-1}$), while the middle and surface had comparatively lower PSR (0.29 m/d $mday^{-1}$ ay and 0.38 $mday^{-1}$). This implies that phytoplankton's sinking rate, carbon flux and total carbon increase with depth.

CHAPTER FIVE: DISCUSSION

The purpose of this research was to create a comprehensive carbon sequestration model covering the entire coastal and maritime region of Bangladesh. To accomplish this, we employed GIS modeling, integrating real-time data and satellite observations.

5.1 Ocean productivity

The findings of this investigation reveal significant variations in the seasonal, and annual concentration of Chl-a near Bangladesh's maritime boundary in the northern Bank of Bangladesh. In this study, the post-monsoon period exhibited the highest Chl-a readings according to MODIS data. In terms of real time data of 2018-19 and 2020-21, the highest value has been obtained in monsoon and post-monsoon. Based on the 2023 data, the concentration of Chl-a was found to fluctuate within the range of 0.28 to 0.67 µg/l. The findings indicated higher concentrations during the post-monsoon season (0.59 µg/l) and lower in the monsoon (0.14 µg/l) (Gopalaksihnan et al., 2020). The current study aligns with the findings of Baliarsingh et al., (2015), conducted in the northwest Bay of Bengal, which reported a concentration range of Chl-a between 0.12 and 10.06 mgm^{-3}. According to the research conducted by Dey et al., 2023, the Chlorophyll-a content exhibited a peak during the northeast monsoon. Subsequently, the content decreased in both the pre-monsoon and post-monsoon periods. During this investigation, the season and station had a substantial impact on the content of chlorophyll-a. The Bay of Bengal (BoB) stands out from other oceans due to its unique regularly reversing monsoon system. As a consequence of this distinctive meteorological pattern, a noticeable seasonal variation in Chl-a levels has been consistently documented throughout the year (Gopalaksihnan et al., 2020 and Vecchi et al., 2002). Additionally, there is a considerable correlation between river runoff and seasonal fluctuations in Chl-a across the northern BoB (Nagamani et al., 2013; Poddar et al., 2019).

As per the findings of this study, the most productive season is the monsoon. The increased wind-driven upwelling along India's eastern coast during the monsoon contributes to the ascent of nutrient-rich waters to the surface. This phenomenon results in increased Chl-a concentrations in the northern BoB region (Chauhan et al., 2001; Baliarsingh et al., 2015). On the contrary, a recent study by Rouf et al., 2020, conducted in the shelf region of the northern BoB over the years 2012-2017, identified a declining trend of Chl-a during the pre-

monsoon. This trend was attributed to decreased wind speed and an increase in temperature during this period. Nagamani et al. 2011 noted the similar pattern for the years 1999-2000. In this study, the Chl-a concentration exhibited an increasing trend starting from the pre-monsoon, reaching its peak in August. However, during August, which typically marks the peak of the monsoon season, there was a significant decline in the onshore concentration of Chl-a. This decline was attributed to reduced light availability caused by increased cloud cover (Gomes et al., 2000). Additionally, rainfall during the monsoon led to increased turbidity (Poddar et al., 2019), which can restrict the ability of phytoplankton to photosynthesize (Sardessai et al., 2007), consequently reducing the amount of Chl-a produced. The onshore region had a substantially larger concentration of Chl-a variability compared to the mid-shore and offshore regions for the annual time series data (2009-10; 2014-15; 2019-20). Indeed, the onshore region is notably vulnerable to changes in sea surface temperature (SST), rainfall, river discharge, nutrient availability, and coastal upwelling. The cumulative impact of these variables can significantly influence the accumulation of phytoplankton overtime, reflecting the interconnected nature of environmental factors in shaping the ecological dynamics of the onshore region (Sardessai et al., 2007; Duofois et al., 2014).

Significant variations in phytoplankton sinking rates (PSR) were observed at different depths, with the monsoon season exhibiting the highest while the pre-monsoon season had the lowest average PSR in the study. In the eastern Indian Ocean, Wang et al. (2022) reported a range of phytoplankton sinking rate from -0.29 to 2.19 md^{-1}, with an average of 0.42±0.65 md^{-1}. The sinking rate is influenced by factors such as plankton density and nutrients availability. Greater depth and reduced surface area were associated with an increase in the sinking rate, as observed in the study. The findings of the current study align with the results of Pearson correlation analysis, revealing a negative association between the sinking rate and temperature and Chl-a, while showing a positive correlation with nutrients. Throughout this investigation, it was discovered that there was a strong correlation between PSR and nutrient contents, and that the sinking rate rose with depth. During the study, the 10 m depth is where the greater PSR was identified. In a related study in the Changjiang Estuary, Guo et al. (2016) examined phytoplankton sinking rate and reported that summertime exhibited a higher sinking rate than spring .

The density of phytoplankton has a profound influence in determining the total carbon content. Phytoplankton cells consist of organic carbon, which actively interacts with the carbon system. Through the biological pump mechanisms, tis carbon is subsequently transported and sequestered into the deep ocean. In the study period, the monsoon and winter seasons exhibited the highest and lowest levels of carbon content respectively. Notably, the Kutubdia station contributed more carbon than Cox's Bazar station. More importantly, the BoB experiences lower carbon concentrations throughout the year due to the persistence of stratification caused by low-speed winds, as indicated by Gauns et al., 2005.

The density of phytoplankton has a profound influence in determining the total carbon content. Phytoplankton cells consist of organic carbon, which actively interacts with the carbon system. Through the biological pump mechanisms, tis carbon is subsequently transported and sequestered into the deep ocean. In the study period, the monsoon and winter seasons exhibited the highest and lowest levels of carbon content respectively. Notably, the Kutubdia station contributed more carbon than Cox's Bazar station. More importantly, the BoB experiences lower carbon concentrations throughout the year due to the persistence of stratification caused by low-speed winds, as indicated by Gauns et al., 2005.

The primary objective of this investigation is to study Carbon Flux (CF). Significant variations in CF were observed with changes in depth. The measured CF ranged between 0.10 to 8.60 mg C $m^{-2}day^{-1}$ during this investigation. The monsoon recorded the highest average whereas the post-monsoon season yielded the lowest. Cox's Bazar station contributes little (1.79 mg C $m^{-2}day^{-}1$)to the carbon flux, while Kutubdia station makes up the majority (2.17 mg C $m^{-2}day^{-1}$). The peak carbon flux was discovered at a depth of 10 meters, and its value varied with depth. Phytoplankton sinking rate correlates with carbon flux. Due to the increased total carbon and phytoplankton sinking rate at this station, there was also a higher carbon flux in Kutubdia. In Changjiang Estuary, a study was carried out by Guo et al., 2016. According to studies, the summer season had a higher carbon flux than the spring season. The summertime carbon flux ranged from 11.90 to 129.69 mg-$Cm^{-2}day^{-1}$ (average = 63.13 ± 48.16 $mgCm^{-2}day^{-1}$), while the springtime carbon flux ranged from 9.29 to 82.44 mg C $m^{-2}day^{-1}$ (average = 26.10 ± 26.25 mg C $m^{-2}day^{-1}$). The yearly mean carbon flux of two stations in the western Pacific varied from 27.3 to 46.7 mg C $m^{-2}day^{-1}$ according

to another study (Honda et al., 2017). Comparing this data to the current study, it was higher. The creation of Subtropical Mode Water (STMW) and the movement of significant volumes of surface water CO_2 into the deep of the ocean are the two main causes of the fluctuation in the western Pacific. In contrast to the current study, the western Pacific exhibited higher nutrients and phytoplankton density. Because of this, the western Pacific has a higher concentration of carbon flow than the Northeastern Bay of Bengal.

5.2 Responses of particulate organic carbon and particulate inorganic carbon

The annual trend reveals substantial and significant changes, providing insights into the inter-annual variability of POC. In this study, monthly surface water POC data from the MODIS satellite were extracted for the year 2009-10, 2014-15, 2019-20. The data were averaged and binned, uncovering the intricate variability in POC concentrations in the northern Bay of Bengal over this three- year dataset. The average POC concentration observed in this study was 177.64 ± 144.61 mgm^{-3}. In comparison, Rouf et al., 2021 reported an average of 153.84 ± 11.17 mgm^{-3} over the period from 2002-2019). A separate study conducted by Stramska et al., 2009 examined significant variations in average POC concentrations across various ocean basins, utilizing a 10-year time series dataset (1998–2007) obtained from SeaWiFS ocean color. The POC concentrations were found to be 45-50 mg m^{-3} on an annual average in the South Pacific, 70-120 mgm^{-3} in the North Atlantic, 58-82 mgm^{-3} in the South Atlantic, 50-85 mgm^{-3} in the North Pacific, 50-100 mgm^{-3} in the Southern Ocean, and 50–75 mgm^{-3} in the Indian Ocean. The global ocean's average POC throughout this 10-year mean time series was 60-75 mgm^{-3}. According to Bhosle et al., 1988, in situ POC studies revealed that POC concentrations in the middle Arabian Sea ranged from 154 to 554 mgm^{-3}.

Fernandes et al. 2009 observed in situ POC along the western BoB ranging from 51.6 to 133.2 mgm^{-3}. In addition, the POC concentration in the southwest BoB, as reported by Kandasamy et al., 2019, ranged from 62.60 to 108.72 mgm^{-3}. The geographic scope of the current study is more limited compared to the broader domains covered in studies by Stramska et al., 2009 and Fernandes et al., 2009, making it more closely associated with terrestrial inputs and coastal systems. This is why POC concentration was found to be substantially greater in the northern BoB. Notably, POC was significantly higher in the

nearshore areas of the northern BoB compared to offshore regions. Consistent with the findings, Fernandes et al., (2009) proposed that river runoff and excessive precipitation over evaporation contribute to freshening the upper water layers, leading to elevated POC concentrations in the BoB, particularly in nearshore area. Gopalakrishna et al. (2002) suggested that the impact of freshwater input is most pronounced near the shore and gradually diminishes towards the offshore regions of the bay. Furthermore, according to Stramska et al., 2009 and Stramska et al., 2005, biological production, carbon pool transformation, and downward export all play roles in influencing POC concentration in surface waters.

The Bay of Bengal (BoB) is characterized by a unique feature known as the monsoon, which plays a defining role in shaping the seasons and influencing key phenomena in the coastal and territorial regions of Bangladesh. Understanding the seasonal variability of particulate organic carbon (POC) allows for insights into how the monsoon impacts POC fluctuations. In the study, it was observed that winter exhibited the highest POC concentrations, measuring at 213.53 ± 152.99 mgm^{-3}. In contrast, Rouf et al., 2021 similarly identified the highest concentration of POC during winter. Similar noteworthy seasonal POC fluctuation was noted in the North Pacific Ocean (Yu et al., 2019), southern ocean (Allison et al., 2010), northern North Atlantic (Stramska et., 2014), Bohai Sea and Yellow Sea (Fan et al., 2018), and western BoB (Fernandes et al., 2009).

The seasonal variations in POC appear to be primarily driven by a combination of factors, including primary productivity, river runoff or terrestrial inputs, eddies pumping, water current, upwelling, reversing monsoon winds, stratification, light availability, and sediment resuspension (Rouf et al., 2021) During the post-monsoon, a moderate POC content of 182.72 ± 159.13 mgm^{-3} was observed. Similar mild POC (90–100 mg m^{-3}) for the southwest BoB during this season were also observed by Kandasamy et al. 2019. Strong stratification (dominated by salinity) in the water column and increased nutrient loading in the surface layer are characteristics of this season, which are marked by high SST (average of 29.27±0.63 ◦C), high wind speed (approximately 10 m/s), and large volume of terrestrial water discharge through the major river systems (Ganga–Brahmaputra–Meghna) (Gomes et al., 2000). Particulate Inorganic Carbon (PIC) makes up roughly one-fourth of all marine

sediments, and its presence extends across both coastal and open ocean regions globally, signifying its significance due to vast magnitude of this carbon pool (Broecker, and Peng, 1982). According to Broecker and Peng 1982, the sedimentary pool of PIC is approximately 5.6 × 106 Pg, which is 7× larger than the sedimentary Particulate Orgaic Carbon pool and 6000× larger than the ocean's Dissolved Organic Carbon pool. The comprehension of PIC concentration in both space and time is of utmost importance due to its significant role in the ocean's carbon cycle, radiative balance, carbon export, and generation of CO_2. In this study, it was observed that both POC and PIC exhibit an increasing trend as the year's progress. The upward trend in both POC and PIC suggests an augmentation in carbon sequestration processes, as indicated by the findings of this study. Particle inorganic carbon (PIC) content is used to evaluate net calcification, while particulate organic carbon (POC) content of coccolithophores is frequently utilized as a measure of net autotrophic productivity. The physiological functioning of coccolithophores can be influenced by environmental conditions, which can alter PIC and POC production. In the context of modeling the oceanic carbon cycle, the ratio of PIC to POC plays a crucial role, offering insights into the export ratio (Ridgwell et al. 2009). Understanding this ratio is essential for gaining a comprehensive understanding of carbon export, carbon flow and sequestration processes and their contribution to the coastal and marine ecosystem.

The results on the seasonal, yearly, and deep changes of Chl-a, and PSR that have been reported make it clear that the dynamics of carbon sequestration processes follow diverse patterns at various temporal and spatial scales. Chl-concentrations showed seasonal variations, with some years showing considerable increases in the spring and gradually rising values in the summer. Winter and summertime POC and PIC trends were rising at the same time, indicating increased carbon sequestration efforts during these times. Over the period of 2009–10 to 2019–20, there was a continuous annual increase in chl-a, which may indicate an amplification in primary productivity. Similarly, rising trends in POC and PIC across these years indicate intensified carbon sequestration processes. The monsoon season particularly highlited heightened carbon sequestration efforts, as evidenced by increasing patterns in Chl-a, TC and PSR metrics. Furthermore, depth-wise analyses unveiled that as one delves into the aquatic environment, there's a notable escalation in phytoplankton sinking rates, carbon flux and total carbon content. This emphasizes the critical role of depth in influencing carbon

sequestration dynamics, with deeper waters potentially serving as significant reservoirs for carbon storage. Collectively, these findings illuminate the multifaceted nature of carbon sequestration processes, influenced by seasonal variations, annual trends, and depth-specific dynamics, underscoring the intricate balance of marine ecosystems in mitigating atmospheric carbon.

CHAPTEER SIX: CONCLUSIONS

This study uses real time data and remotely sensed data to illustrate the seasonal and annual fluctuation of Chl-a, POC, PIC, CF, TC, PSR in the Northern Bay of Bengal. The results revealed that the annual average of 3-years (2009-10, 2014-15, 2019-20) surface POC average concentration 144.62±177.64 mgm^{-3} observed in the Northern Bay of Bengal. The average concentration of PIC 0.05±0.13 mgm^{-3} and Chl-a 1.93±2.87 mgm^{-3} also identified. Carbon sinking occurs in the northeastern Bay of Bengal in considerable amounts, according to real-time data. Throughout the monsoon season, the greatest carbon flux was recorded; this fluctuated with depth. Plankton density and carbon content both contribute significantly to carbon flux and are observed to be higher during the monsoon season. The real-time data and the MODIS data were shown to have a somewhat good relationship. This work may be provide as baseline data for future research on the health and dynamics of the northern BoB's ocean ecosystem. It is the first attempt to examine the yearly and seasonal trend of Chl-a, PSR in the region and to make a relationship between real time data and MODIS data. To guarantee the accuracy of MODIS data, however, a thorough investigation is still required through regional algorithm inversion or correction. Further research into the vertical and spatial profile of Carbon stock is required in order to fully understand the dynamics of Carbon sinking and its underlying mechanisms in the northern BoB. The techniques and information from this study are valuable for future research on carbon stock estimation in other coastal systems. Lastly, by providing information on carbon sequestration in coastal systems, this research will help manage our fisheries stock and lessen the impact of climate change.

CHAPTER SEVEN: REFERENCES

Allenby, B.R. (2002). Global climate change and the anthropogenic earth. The carbon dioxide dilemma: Promising technologies and policies. The national academies press, NRC (National Research Council), Washington DC.

Allison, D. B., Stramski, D., & Mitchell, B. G. (2010). Seasonal and interannual variability of particulate organic carbon within the Southern Ocean from satellite ocean color observations. Journal of Geophysical Research: Oceans, 115(C6).

Althoff, P., & Chandler, D. E. (1999). Carbon inventory in a Eucalyptus camaldulensis plantation compared with natural vegetation in Brazil. Field Tests of Carbon Monitoring Methods in Forestry Projects. Forest Carbon Monitoring Program. Winrock International Institute for Agricultural Development, 3-15.

Anzecc, A. (2000). Australian and New Zealand guidelines for fresh and marine water quality. Australian and New Zealand Environment and Conservation Council and Agriculture and Resource Management Council of Australia and New Zealand, Canberra, 1, 1-314.

Archer, D., Kheshgi, H., & Maier-Reimer, E. (1997). Multiple timescales for neutralization of fossil fuel CO_2. Geophysical Research Letters, 24(4), 405-408.

Aze, T., Barry, J., Bellerby, R. G., Brander, L., Byrne, M., Dupont, S., ... & Young, J. R. (2014). An updated synthesis of the impacts of ocean acidification on marine biodiversity (CBD Technical Series; 75). Secretariat of the Convention on Biological Diversity.

Baliarsingh, S. K., Lotliker, A. A., Sahu, K. C., & Sinivasa Kumar, T. (2015). Spatio-temporal distribution of chlorophyll-a in relation to physico-chemical parameters in coastal waters of the northwestern Bay of Bengal. Environmental monitoring and assessment, 187, 1-14.

Baliarsingh, S. K., Lotliker, A. A., Sahu, K. C., & Sinivasa Kumar, T. (2015). Spatio-temporal distribution of chlorophyll-a in relation to physico-chemical parameters in coastal waters of the northwestern Bay of Bengal. Environmental monitoring and assessment, 187, 1-14.

Basu S, Mackey KR. (2018). Phytoplankton as key mediators of the biological carbon pump: Their responses to a changing climate. Sustainability, 10(3): 869.

Behrenfeld, M. J., Boss, E., Siegel, D. A., & Shea, D. M. (2005). Carbon-based ocean productivity and phytoplankton physiology from space. Global biogeochemical cycles, 19(1).

Behrenfeld, M. J., Hu, Y., Hostetler, C. A., Dall'Olmo, G., Rodier, S. D., Hair, J. W., & Trepte, C. R. (2013). Space-based lidar measurements of global ocean carbon stocks. Geophysical Research Letters, 40(16), 4355-4360.

Bhosle, N. B., Dhople, V. M., & Wagh, A. B. (1988). Distribution of particulate organic carbon in the central Arabian Sea. Proceedings of the Indian Academy of Sciences-Earth and Planetary Sciences, 97, 35-47.

Broecker, W. S., & Peng, T. H. (1982). Tracers in the Sea (Vol. 690). Palisades, New York: Lamont-Doherty Geological Observatory, Columbia University. Gomes, H. R., Goes, J. I., & Saino, T. (2000). Influence of physical processes and freshwater discharge on the seasonality of phytoplankton regime in the Bay of Bengal. Continental Shelf Research, 20(3), 313-330.

Broecker, W. S., Takahashi, T., Andersen, N. R., & Malahoff, A. (1977). Neutralization of fossil fuel CO_2 by marine calcium carbonate.

Burdige, D. J. (2007). Preservation of organic matter in marine sediments: controls, mechanisms, and an imbalance in sediment organic carbon budgets?. Chemical reviews, 107(2), 467-485.

Caldeira, K., & Wickett, M. E. (2003). Anthropogenic carbon and ocean pH. Nature, 425(6956), 365-365.

Chauhan, P., Nagur, C. R. C., Mohan, M., Nayak, S. R., & Navalgund, R. R. (2001). Surface chlorophyll-a distribution in Arabian Sea and Bay of Bengal using IRS-P4 Ocean Colour Monitor satellite data. Current science, 80(2), 127-129.

Chow, A. (2014). Ocean carbon sequestration by direct injection. In CO2 Sequestration and Valorization. London, UK: IntechOpen.

Daggash, H. A. (2021). Are the IPCC's findings encouraging climate action in sub-Saharan Africa?. Joule, 5(10), 2540-2542.

De la Rocha, C., & Passow, U. (2014). The biological pump.

Dey S, Singh RP. (2003). Comparison of chlorophyll distributions in the northeastern Arabian Sea and southern Bay of Bengal using IRS-P4 Ocean Color Monitor data. Remote Sensing of Environment, 85(4): 424-428.

Dufois, F., Hardman-Mountford, N. J., Greenwood, J., Richardson, A. J., Feng, M., Herbette, S., & Matear, R. (2014). Impact of eddies on surface chlorophyll in the S outh I ndian O cean. Journal of Geophysical Research: Oceans, 119(11), 8061-8077.

Duforêt-Gaurier, L., Loisel, H., Dessailly, D., Nordkvist, K., & Alvain, S. (2010). Estimates of particulate organic carbon over the euphotic depth from in situ measurements. Application to satellite data over the global ocean. Deep Sea Research Part I: Oceanographic Research Papers, 57(3), 351-367.

Estes, N. (2019). Our history is the future: Standing Rock versus the Dakota Access Pipeline, and the long tradition of indigenous resistance. Verso Books. Mcleod, E., Chmura, G. L., Bouillon, S., Salm, R., Björk, M., Duarte, C. M., ... & Silliman, B. R. (2011). A blueprint for blue carbon: toward an improved understanding of the role of vegetated coastal habitats in sequestering CO2. Frontiers in Ecology and the Environment, 9(10), 552-560.

Evers-King, H., Martinez-Vicente, V., Brewin, R. J., Dall'Olmo, G., Hickman, A. E., Jackson, T., ... & Sathyendranath, S. (2017). Validation and intercomparison of ocean color algorithms for estimating particulate organic carbon in the oceans. Frontiers in Marine Science, 251.

Falloon, P. D., Smith, P., Smith, J. U., Szabo, J., Coleman, K., & Marshall, S. (1998). Regional estimates of carbon sequestration potential: linking the Rothamsted Carbon Model to GIS databases. Biology and Fertility of soils, 27(3), 236-241.

Fan, H., Wang, X., Zhang, H., & Yu, Z. (2018). Spatial and temporal variations of particulate organic carbon in the Yellow-Bohai Sea over 2002–2016. Scientific Reports, 8(1), 7971.

Fernandes, L., Bhosle, N. B., Matondkar, S. P., & Bhushan, R. (2009). Seasonal and spatial distribution of particulate organic matter in the Bay of Bengal. Journal of Marine Systems, 77(1-2), 137-147.

Freund, P., & Ormerod, W. G. (1997). Progress toward storage of carbon dioxide. Energy Conversion and Management, 38, S199-S204.

Friedlingstein P, O'Sullivan M, Jones Andrew Hauck J et al. (2020). Global carbon budget 2020. Earth Syst. Sci. Data 12: 3269–340

Gardner, W. D., Mishonov, A. V., & Richardson, M. J. (2006). Global POC concentrations from in-situ and satellite data. Deep Sea Research Part II: Topical Studies in Oceanography, 53(5-7), 718-740.

Gauns M, Madhupratap M, Ramaiah N, Jyothibabu R, Fernandes V, Paul Kumar SP. 2005. Comparative accounts of biological productivity characteristics and estimates of carbon fluxes in the Arabian Sea and the Bay of Bengal. Deep Sea Research Part II: Topical Studies in Oceanography: 1;52(14-15):2003-17.

George, M. D., Kumar, M. D., Naqvi, S. W. A., Banerjee, S., Narvekar, P. V. and co-authors, (1994). A study of the carbon dioxide system in the northern Indian Ocean during premonsoon. Mar. Chem. 47, 243254. https://doi.org/10.1016/0304-4203(94)90023-X

Giri, R. K. K. V., & Madla, V. R. (2017). Study and Evaluation of Carbon Sequestration using Remote Sending and GIS: A Review on Various Techniques. International Journal of Civil Engineering and Technology, 8(4), 287-300.

Gomes, H. R., Goes, J. I., & Saino, T. (2000). Influence of physical processes and freshwater discharge on the seasonality of phytoplankton regime in the Bay of Bengal. Continental Shelf Research, 20(3), 313-330.

Gopalakrishna, V. V., Murty, V. S. N., Sengupta, D., Shenoy, S., & Araligidad, N. (2002). Upper ocean stratification and circulation in the northern Bay of Bengal during southwest monsoon of 1991. Continental Shelf Research, 22(5), 791-802.

Gopalakrishnan, G., Subramanian, A. C., Miller, A. J., Seo, H., & Sengupta, D. (2020). Estimation and prediction of the upper ocean circulation in the Bay of Bengal. Deep Sea Research Part II: Topical Studies in Oceanography, 172, 104721.

Gower, S. T. (2003). Patterns and mechanisms of the forest carbon cycle. Annual Review of Environment and Resources, 28(1), 169-204.

Guo S, Sun J, Zhao Q, Feng Y, Huang D, Liu S. (2016). Sinking rates of phytoplankton in the Changjiang (Yangtze River) estuary: A comparative study between Prorocentrum dentatum and Skeletonema dorhnii bloom. Journal of Marine Systems, 154, 5-14.

Haywood, J., & Schulz, M. (2007). Causes of the reduction in uncertainty in the anthropogenic radiative forcing of climate between IPCC (2001) and IPCC (2007). Geophysical Research Letters, 34(20).

Hedges, J. I., & Keil, R. G. (1995). Sedimentary organic matter preservation: an assessment and speculative synthesis. Marine chemistry, 49(2-3), 81-115.

Hegde, A. A., Pruthviraj, U., & Shetty, A. (2019). A QGIS Plug-in for Processing MODIS Data. In 2019 IEEE 5th International Conference for Convergence in Technology (I2CT) (pp. 1-4). IEEE.

Herr, D., & Landis, E. (2016). Coastal blue carbon ecosystems. Opportunities for Nationally Determined Contributions. Policy Brief.

Herzog, H., Caldeira, K., & Reilly, J. (2003). An issue of permanence: Assessing the effectiveness of temporary carbon storage. Climatic Change, 59(3), 293-310.

Herzog, H., Drake, E., & Adams, E. (1997). CO Capture, Reuse, and Storage Technologies. Citeseer1997.

Hoffert, M. I., Wey, Y. C., Callegari, A. J., & Broecker, W. S. (1979). Atmospheric response to deep-sea injections of fossil-fuel carbon dioxide. Climatic Change, 2(1), 53-68.

Honda Wakita M, Matsumoto K, Fujiki T, Siswanto E, Sasaoka K, Saino T. (2017). Comparison of carbon cycle between the western Pacific subarctic and subtropical time-series stations: highlights of the K2S1 project. Journal of Oceanography, 73(5): 647-667.

Hood, E., Battin, T. J., Fellman, J., O'neel, S., & Spencer, R. G. (2015). Storage and release of organic carbon from glaciers and ice sheets. Nature geoscience, 8(2), 91-96.

Howard, E. A., Gower, S. T., Foley, J. A., & Kucharik, C. J. (2004). Effects of logging on carbon dynamics of a jack pine forest in Saskatchewan, Canada. Global Change Biology, 10(8), 1267-1284.

Hu, C., Lee, Z., & Franz, B. (2012). Chlorophyll aalgorithms for oligotrophic oceans: A novel approach based on three-band reflectance difference. Journal of Geophysical Research: Oceans, 117(C1).

Hu, S. B., Cao, W. X., Wang, G. F., Xu, Z. T., Lin, J. F., Zhao, W. J., ... & Yao, L. J. (2016). Comparison of SeaWiFS-derived particulate organic carbon, and in situ measurements in the South China Sea. International Journal of Remote Sensing, 37(7), 1585-1600.

Jewel Haque Haq Khan S. (2002). Seasonal dynamics of phytoplankton in relation to environmental factors in the Maheshkhali channel, Cox's Bazar, Bangladesh.

Jiao, N., Robinson, C., Azam, F., Thomas, H., Baltar, F., Dang, H., ... & Zhang, R. (2014). Mechanisms of microbial carbon sequestration in the ocean–future research directions. Biogeosciences, 11(19), 5285-5306.

Joos, F., Prentice, I. C., Sitch, S., Meyer, R., Hooss, G., Plattner, G. K., ... & Hasselmann, K. (2001). Global warming feedbacks on terrestrial carbon uptake under the Intergovernmental Panel on Climate Change (IPCC) emission scenarios. Global Biogeochemical Cycles, 15(4), 891-907.

Joos, F., Prentice, I. C., Sitch, S., Meyer, R., Hooss, G., Plattner, G. K., ... & Hasselmann, K. (2001). Global warming feedbacks on terrestrial carbon uptake under the Intergovernmental Panel on Climate Change (IPCC) emission scenarios. Global Biogeochemical Cycles, *15*(4), 891-907.

Kandasamy, P., Sarangi, R. K., Ayyappan, S., Allimuthu, D., Ramalingam, S., & Durairaj, P. (2019). Influence of sea surface temperature and chlorophyll-a on the distribution of particulate organic carbon in the southwest Bay of Bengal. J. Geomatics, 13, 291-303.

King, J. S., Kubiske, M. E., Pregitzer, K. S., Hendrey, G. R., McDonald, E. P., Giardina, C. P., ... & Karnosky, D. F. (2005). Tropospheric O3 compromises net primary production in young stands of trembling aspen, paper birch and sugar maple in response to elevated atmospheric CO2. New Phytologist, 168(3), 623-636.

Koss, P. A., Martin, D., & Oehmichen, W. (2007). Factors Associated with Carbon Sequestration. Unpublished manuscript University of Wisconsin, available at: www. uwgb. edu/fermanik/ES_P763/Carbon_sequestration_factors_poster_ESP2007. pdf.

Kumar, M. D., Naqvi, S. W. A., George, M. D., & Jayakumar, D. A. (1996). A sink for atmospheric carbon dioxide in the northeast Indian Ocean. Journal of Geophysical Research: Oceans, 101(C8), 18121-18125.

Kumar, S., & Ramkrishna, D. (1996). On the solution of population balance equations by discretization—II. A moving pivot technique. Chemical Engineering Science, 51(8), 1333-1342.

Lackner, K. S. (2002). Carbonate chemistry for sequestering fossil carbon. Annual review of energy and the environment, 27(1), 193-232.

Lackner, K. S., Park, A. H. A., & Miller, B. G. (2010). Eliminating CO_2 emissions from coal-fired power plants. Generating Electricity in a Carbon-Constrained World, 127-173.

Lal, R. (1998). Soil erosion impact on agronomic productivity and environment quality. Critical reviews in plant sciences, 17(4), 319-464.

Lal, R. (2008). Carbon sequestration. Philosophical Transactions of the Royal Society B: Biological Sciences, 363(1492), 815-830.

Lavery, T. J., Roudnew, B., Gill, P., Seymour, J., Seuront, L., Johnson, G., ... & Smetacek, V. (2010). Iron defecation by sperm whales stimulates carbon export in the Southern Ocean. Proceedings of the Royal Society B: Biological Sciences, 277(1699), 3527-3531.

Le, C., Lehrter, J. C., Hu, C., MacIntyre, H., & Beck, M. W. (2017). Satellite observation of particulate organic carbon dynamics on the L ouisiana continental shelf. Journal of Geophysical Research: Oceans, 122(1), 555-569.

Lee, D., Son, S., Joo, H., Kim, K., Kim, M. J., Jang, H. K., ... & Lee, S. H. (2020). Estimation of the particulate organic carbon to chlorophyll-a ratio using MODIS-Aqua in the East/Japan Sea, South Korea. Remote Sensing, 12(5), 840.

Liu, D., Pan, D., Bai, Y., He, X., Wang, D., Wei, J. A., & Zhang, L. (2015). Remote sensing observation of particulate organic carbon in the Pearl River Estuary. Remote Sensing, 7(7), 8683-8704.

Liu, Z., Robinson, J. T., Sun, X., & Dai, H. (2008). PEGylated nanographene oxide for delivery of water-insoluble cancer drugs. Journal of the American Chemical Society, 130(33), 10876-10877.

Loisel, H., Bosc, E., Stramski, D., Oubelkheir, K., & Deschamps, P. Y. (2001). Seasonal variability of the backscattering coefficient in the Mediterranean Sea based on satellite SeaWiFS imagery. Geophysical Research Letters, 28(22), 4203-4206.

Lovelock, C. E., Atwood, T., Baldock, J., Duarte, C. M., Hickey, S., Lavery, P. S., ... & Steven, A. (2017). Assessing the risk of carbon dioxide emissions from blue carbon ecosystems. Frontiers in Ecology and the Environment, 15(5), 257-265.

Mahmood, H., Siddique, M. R. H., & Akhter, M. (2016). A critical review and database of biomass and volume allometric equation for trees and shrubs of Bangladesh. In IOP Conference Series: Earth and Environmental Science (Vol. 39, No. 1, p. 012057).

Majumder, S. C., Islam, K., & Hossain, M. M. (2019). State of research on carbon sequestration in Bangladesh: a comprehensive review. Geology, Ecology, and Landscapes, 3(1), 29-36. https://doi.org/10.1080/24749508.2018.1481656

Marchetti, C. (1977). On geoengineering and the CO_2 problem. Climatic change, 1(1), 59-68.

Mcleod, E., Chmura, G. L., Bouillon, S., Salm, R., Björk, M., Duarte, C. M., ... & Silliman, B. R. (2011). A blueprint for blue carbon: toward an improved understanding of the role of

vegetated coastal habitats in sequestering CO_2. Frontiers in Ecology and the Environment, 9(10), 552-560.

Metz, B., Davidson, O., & De Coninck, H. (Eds.). (2005). Carbon dioxide capture and storage: special report of the intergovernmental panel on climate change. Cambridge University Press.

Phan, V. H., Pham, D. P. H., Pham, T. V., Qureshi, K. N., & Pham-Quoc, C. (2023). An IoT System and MODIS Images Enable Smart Environmental Management for Mekong Delta. Future Internet, 15(7), 245.

Nagamani, P. V., Hussain, M. I., Choudhury, S. B., Panda, C. R., Sanghamitra, P., Kar, R. N., ... & Rao, K. H. (2013). Validation of chlorophyll-a algorithms in the coastal waters of Bay of Bengal initial validation results from OCM-2. Journal of the Indian Society of Remote Sensing, 41, 117-125.

Nagamani, P. V., Shikhakolli, R., & Chauhan, P. (2011). Phytoplankton variability in the Bay of Bengal during winter monsoon using Oceansat-1 Ocean Colour Monitor data. Journal of the Indian Society of Remote Sensing, 39, 117-126.

Ortega, A., Geraldi, N. R., Alam, I., Kamau, A. A., Acinas, S. G., Logares, R., ... & Duarte, C. M. (2019). Important contribution of macroalgae to oceanic carbon sequestration. Nature Geoscience, 12(9), 748-754.

Passow, U., & Carlson, C. A. (2012). The biological pump in a high CO_2 world. Marine Ecology Progress Series, 470, 249-271.

Pendleton, L., Donato, D. C., Murray, B. C., Crooks, S., Jenkins, W. A., Sifleet, S., ... & Baldera, A. (2012). Estimating global “blue carbon” emissions from conversion and degradation of vegetated coastal ecosystems.

Poddar, S., Chacko, N., & Swain, D. (2019). Estimation of Chlorophyll-a in northern coastal Bay of Bengal using Landsat-8 OLI and Sentinel-2 MSI sensors. Frontiers in Marine Science, 6, 598.

Polimene, L., Sailley, S., Clark, D., Mitra, A., & Allen, J. I. (2017). Biological or microbial carbon pump? The role of phytoplankton stoichiometry in ocean carbon sequestration. Journal of Plankton Research, 39(2), 180-186.

Pussinen, A., Karjalainen, T., Kellomäki, S., & Mäkipää, R. (1997). Potential contribution of the forest sector to carbon sequestration in Finland. Biomass and Bioenergy, 13(6), 377-387.

Qian, Y. L., Bandaranayake, W., Parton, W. J., Mecham, B., Harivandi, M. A., & Mosier, A. R. (2003). Long-term effects of clipping and nitrogen management in turfgrass on soil organic carbon and nitrogen dynamics: The CENTURY model simulation. Journal of Environmental Quality, 32(5), 1694-1700.

Rao, C. K., Naqvi, S. W. A., Kumar, M. D., Varaprasad, S. J. D., Jayakumar, D. A. and co-authors, (1994). Hydrochemistry of the Bay of Bengal: possible reasons for a differentwater-column cycling of carbon and nitrogen from the Arabian Sea. Mar. Chem. 47, 279290.

Ridgwell, A., Schmidt, D. N., Turley, C., Brownlee, C., Maldonado, M. T., Tortell, P., & Young, J. R. (2009). From laboratory manipulations to Earth system models: scaling calcification impacts of ocean acidification. Biogeosciences, 6(11), 2611-2623.

Rouf, M. A., Antu, A. H., & Noor, I. (2020). Seasonal and annual variability in chlorophyll-in the shelf region of the Northern Bay of Bengal using MODIS-Aqua data. Oceanological and Hydrobiological Studies, 49(4), 398-407.

Rouf, M. A., Golder, M. R., & Sumana, Z. A. (2021). Satellite-based observation of particulate organic carbon in the northern Bay of Bengal. Environmental Advances, 6, 100124.

Roy, R., Vinayachandran, P. N., Sarkar, A., George, J., Parida, C., Lotliker, A., ... & Choudhury, S. B. (2021). Southern Bay of Bengal: A possible hotspot for CO2 emission during the summer monsoon. Progress in Oceanography, 197, 102638.

Saatchi, S. S., Harris, N. L., Brown, S., Lefsky, M., Mitchard, E. T., Salas, W., ... & Morel, A. (2011). Benchmark map of forest carbon stocks in tropical regions across three continents. Proceedings of the national academy of sciences, 108(24), 9899-9904.

Sardessai, S., Ramaiah, N., Prasanna Kumar, S., & De Sousa, S. N. (2007). Influence of environmental forcings on the seasonality of dissolved oxygen and nutrients in the Bay of Bengal. Journal of Marine Research, 65(2), 301-316.

Sarma, V. V. S. S., Krishna, M. S., Rao, V. D., Viswanadham, R., Kumar, N. A., Kumari, T. R., ... & Tari, A. (2012). Sources and sinks of CO2 in the west coast of Bay of Bengal. Tellus B: Chemical and Physical Meteorology, 64(1), 10961.

Shawal, S., Shoyab, M., & Begum, S. (2014). Fundamentals of digital image processing and basic concept of classification. International Journal of Chemical and Process Engineering Research, 1(6), 98-108.

Shawal, S., Shoyab, M., & Begum, S. (2014). Fundamentals of digital image processing and basic concept of classification. International Journal of Chemical and Process Engineering Research, 1(6), 98-108.

Shetye, S. R., Gouveia, A. D., Shankar, D., Shenoi, S. S. C., Vinayachandran, P. N., Sundar, D., ... & Nampoothiri, G. (1996). Hydrography and circulation in the western Bay of Bengal during the northeast monsoon. Journal of Geophysical Research: Oceans, 101(C6), 14011-14025.

Shin, M. Y., Miah, M. D., & Lee, K. H. (2007). Potential contribution of the forestry sector in Bangladesh to carbon sequestration. Journal of environmental management, 82(2), 260-276.

Sloan, E. D. (2003). Fundamental principles and applications of natural gas hydrates. Nature, 426(6964), 353-359.

Solomon, S. (2007, December). IPCC (2007): Climate change the physical science basis. In Agu fall meeting abstracts (Vol. 2007, pp. U43D-01).

Stramska, M. (2009). Particulate organic carbon in the global ocean derived from SeaWiFS ocean color. Deep Sea Research Part I: Oceanographic Research Papers, 56(9), 1459-1470.

Stramska, M. (2014). Particulate organic carbon in the surface waters of the North Atlantic: spatial and temporal variability based on satellite ocean colour. International Journal of Remote Sensing, 35(13), 4717-4738.

Stramska, M., & Stramski, D. (2005). Variability of particulate organic carbon concentration in the north polar Atlantic based on ocean color observations with Sea-viewing Wide Field-of-view Sensor (SeaWiFS). Journal of Geophysical Research: Oceans, 110(C10).

Stramska, M., Stramski, D., Kaczmarek, S., Allison, D. B., & Schwarz, J. (2006). Seasonal and regional differentiation of bio-optical properties within the north polar Atlantic. Journal of Geophysical Research: Oceans, 111(C8).

Stramski, D., Joshi, I., & Reynolds, R. A. (2022). Ocean color algorithms to estimate the concentration of particulate organic carbon in surface waters of the global ocean in support of a long-term data record from multiple satellite missions. Remote Sensing of Environment, 269, 112776.

Stramski, D., Reynolds, R. A., Babin, M., Kaczmarek, S., Lewis, M. R., Röttgers, R., ... & Claustre, H. (2008). Relationships between the surface concentration of particulate organic carbon and optical properties in the eastern South Pacific and eastern Atlantic Oceans. Biogeosciences, 5(1), 171-201.

Stramski, D., Reynolds, R. A., Kahru, M., & Mitchell, B. G. (1999). Estimation of particulate organic carbon in the ocean from satellite remote sensing. Science, 285(5425), 239-242.

Sverdrup, H. U., Johnson, M. W., & Fleming, R. H. (1942). The Oceans: Their physics, chemistry, and general biology (Vol. 1087). New York: Prentice-Hall.

Takahashi, T., Sutherland, S. C., Wanninkhof, R., Sweeney, C., Feely, R. A., Chipman, D. W., ... & De Baar, H. J. (2009). Climatological mean and decadal change in surface ocean pCO_2, and net sea–air CO_2 flux over the global oceans. Deep Sea Research Part II: Topical Studies in Oceanography, 56(8-10), 554-577.

Takahashi, T., Sutherland, S. C., Wanninkhof, R., Sweeney, C., Feely, R. A., Chipman, D. W., ... & De Baar, H. J. (2009). Climatological mean and decadal change in surface ocean pCO_2, and net sea–air CO_2 flux over the global oceans. Deep Sea Research Part II: Topical Studies in Oceanography, 56(8-10), 554-577.

Temple, James (September 19, 2021). "Companies hoping to grow carbon-sucking kelp may be rushing ahead of the science". MIT Technology Review. Archived from the original on September 19, 2021. Retrieved November 25, 2021.

Tennen, H., Affleck, G., Coyne, J. C., Larsen, R. J., & DeLongis, A. (2006). Paper and plastic in daily diary research: Comment on Green, Rafaeli, Bolger, Shrout, and Reis (2006).

Thusoo, A., Sarma, J. S., Jain, N., Shao, Z., Chakka, P., Anthony, S., ... & Murthy, R. (2009). Hive: a warehousing solution over a map-reduce framework. Proceedings of the VLDB Endowment, 2(2), 1626-1629.

Tim, N., Zorita, E., & Hünicke, B. (2015). Decadal variability and trends of the Benguela upwelling system as simulated in a high-resolution ocean simulation. Ocean Science, 11(3), 483-502.

Toutin, T. (2004). Geometric processing of remote sensing images: models, algorithms and methods. International journal of remote sensing, 25(10), 1893-1924.

Toutin, T. (2004). Geometric processing of remote sensing images: models, algorithms and methods. International journal of remote sensing, 25(10), 1893-1924.

Tsunogai, S., Watanabe, S., & Sato, T. (1999). Is there a “continental shelf pump” for the absorption of atmospheric CO2?. Tellus B: Chemical and Physical Meteorology, 51(3), 701-712.

USGS (2023) What is carbon sequestration? Energy- US Department of the Interior, USA (Accessed October 08, 2023)

Varkey, M. J., Murty, V. S. N., & Suryanarayana, A. (1996). Physical oceanography of the Bay of Bengal and Andaman Sea. Oceanography and marine biology: an annual review.

Vecchi, G. A., & Harrison, D. E. (2002). Monsoon breaks and subseasonal sea surface temperature variability in the Bay of Bengal. Journal of climate, 15(12), 1485-1493.

Wang, M., & Son, S. (2016). VIIRS-derived chlorophyll-a using the ocean color index method. Remote sensing of Environment, 182, 141-149.

Yu, J., Wang, X., Fan, H., & Zhang, R. H. (2019). Impacts of physical and biological processes on spatial and temporal variability of particulate organic carbon in the North Pacific Ocean during 2003–2017. Scientific Reports, 9(1), 16493.

APPENDICES: APPENDIX

Table 2 *Chlorophyll-a concentration of Bangladesh EEZ (2009-2010)*

Chl-a Concentration (2009-10)							
Season	**Highly Productive Zone**		**Moderately Productive Zone**		**Less Productive Zone**		**Concentration (mg/m3)**
	Area (Sq km)	**%**	**Area (Sq km)**	**%**	**Area (Sq km)**	**%**	
Winter	7,480	7.71	20,752.34	21.38	68,838.22	70.92	1.38 ± 1.66
Pre-monsoon	1,013.46	1.09	16,460.62	17.85	74,766.96	81.06	2.07 ± 5.11
Monsoon	5,247.89	6.25	14,354.83	17.09	64,413.81	76.67	1.17± 2.05
Post-monsoon	11,855	12.49	16,352.22	17.24	66,658.75	70.27	1.58 ± 2.17

Table 3 *Chlorophyll-a concentration of Bangladesh EEZ (2014-2015)*

Chl-a Concentration (2014-15)							
Season	**Highly Productive Zone**		**Moderately Productive Zone**		**Less Productive Zone**		**Concentration (mg/m3)**
	Area (Sq km)	**%**	**Area (Sq km)**	**%**	**Area (Sq km)**	**%**	
Winter	5,503	5.39	25,862.94	25.37	70,573.88	69.23	1.32 ± 1.66
Pre-monsoon	13,406.07	13.91	16,029.28	16.63	66,932.38	69.46	1.18 ± 1.61
Monsoon	4,616.59	5.36	11,802.27	13.71	69,642.82	80.92	1.11 ± 1.79
Post-monsoon	10,670	11.33	15,725.93	16.69	67,790.00	71.97	1.51 ± 1.97

Table 4 *Chlorophyll-a concentration of Bangladesh EEZ (2019-2020)*

Chl-a Concentration (2019-20)							
Season	**Highly Productive Zone**		**Moderately Productive Zone**		**Less Productive Zone**		**Concentration (mg/m3)**
	Area (Sq km)	**%**	**Area (Sq km)**	**%**	**Area (Sq km)**	**%**	
Winter	1,656	1.72	27,783.19	28.82	66,948.51	69.46	1.93 ± 2.35
Pre-monsoon	5,868.82	6.59	15,972.94	17.94	67,187.56	75.47	3.75± 5.64
Monsoon	10,845.17	15.99	7,530.51	11.11	49.422.56	72.89	2.56 ± 3.32
Post-monsoon	9,723	10.12	18,045.11	18.79	68,284.59	71.09	3.58 ± 4.77

Table 5 *POC concentration of Bangladesh EEZ (2009-2010)*

POC Concentration (2009-10)							
Season	**Highly Productive Zone**		**Moderately Productive Zone**		**Less Productive Zone**		**Concentration (mg/m3)**
	Area (Sq km)	**%**	**Area (Sq km)**	**%**	**Area (Sq km)**	**%**	
Winter	23,343	24.2	10,560.10	10.9	62,581.21	67.9	195.4 ± 160.1
Pre-monsoon	16,270.70	19.5	25,391.50	30.4	41,801.60	50.1	226.1 ± 187.6
Monsoon	17,191.40	20.9	8,583.60	10.4	56,371.50	68.6	135.2 ± 123.8
Post-monsoon	23,669	28.1	10,258.90	12.5	63,046.20	76.7	178.8 ± 160.8

Table 6 *POC concentration of Bangladesh EEZ (2014-2015)*

POC Concentration (2014-15)							
Season	**Highly Productive Zone**		**Moderately Productive Zone**		**Less Productive Zone**		**Concentration (mg/m3)**
	Area (Sq km)	**%**	**Area (Sq km)**	**%**	**Area (Sq km)**	**%**	
Winter	10,157	10.7	20,762.04	21.9	63,762.50	67.3	175.3 ± 142.1
Pre-monsoon	24,166.70	26.4	5,393.90	5.9	61,850.75	67.6	151.6 ± 131.9
Monsoon	8,064.60	9.4	13,417.80	15.7	64,245.90	74.9	146.5 ± 107.3
Post-monsoon	18,098	19.7	10,244.90	10.04	64,712.60	70.3	177.6 ± 157.1

Table 7 *POC concentration of Bangladesh EEZ (2019-2020)*

POC Concentration (2019-20)							
Season	**Highly Productive Zone**		**Moderately Productive Zone**		**Less Productive Zone**		**Concentration (mg/m3)**
	Area (Sq km)	**%**	**Area (Sq km)**	**%**	**Area (Sq km)**	**%**	
Winter	25,028	27.07	8,970.70	9.7	58,450.20	63.2	231 ± 156.8
Pre-monsoon	19,779.64	21.4	12,079.30	13.1	60,383.10	65.5	164.6 ± 131.6
Monsoon	25,643.30	33.1	12,498.90	16.2	39,245.10	50.7	154.8 ± 116.729
Post-monsoon	26,990	28.04	10,467.04	10.9	58,774.10	61.1	191.8 ± 159.5

Table 8 *PIC concentration of Bangladesh EEZ (2009-2010)*

PIC Concentration (2009-10)							
Season	**Highly Productive Zone**		**Moderately Productive Zone**		**Less Productive Zone**		**Concentration (mg/m3)**
	Area (Sq km)	**%**	**Area (Sq km)**	**%**	**Area (Sq km)**	**%**	
Winter	607	1.89	1,014.22	3.17	30,397.26	94.94	0.001 ± 0.007
Pre-monsoon	263.22	0.38	870.51	1.24	69,083.01	98.39	0.001 ± 0.001
Monsoon	1,422.01	1.79	4,797.48	6.06	72,944.43	92.14	0.003 ± 0.011
Post-monsoon	1,919	2.26	3,902.66	4.59	79,224.99	93.15	0.002 ± 0.008

Table 9 *PIC concentration of Bangladesh EEZ (2014-2015)*

PIC Concentration (2014-15)							
Season	**Highly Productive Zone**		**Moderately Productive Zone**		**Less Productive Zone**		**Concentration (mg/m3)**
	Area (Sq km)	**%**	**Area (Sq km)**	**%**	**Area (Sq km)**	**%**	
Winter	249	0.26	12,132.46	12.5	84,660.93	87.24	0.58 ± 1.34
Pre-monsoon	223.58	0.26	1,868.69	2.21	82,554.49	97.53	0.001± 0.005
Monsoon	157.71	0.19	1,413.64	1.79	77,327.96	98.008	0.0009 ± 0.0035
Post-monsoon	244	0.29	3,731.86	4.44	80,096.44	95.27	0.001 ± 0.006

Table 10 *PIC concentration of Bangladesh EEZ (2019-2020)*

PIC Concentration (2019-20)							
Season	**Highly Productive Zone**		**Moderately Productive Zone**		**Less Productive Zone**		**Concentration (mg/m3)**
	Area (Sq km)	**%**	**Area (Sq km)**	**%**	**Area (Sq km)**	**%**	
Winter	393	0.46	1,457.51	1.72	82,995.84	97.82	0.0009 ± 0.0041
Pre-monsoon	735.34	0.86	2,096.61	2.46	82,418.37	96.68	0.001 ± 0.005
Monsoon	1,988.52	2.59	2,886.31	3.77	71,775.03	93.64	0.003 ± 0.009
Post-monsoon	1,645	1.97	6,393.12	7.66	75,423.75	90.37	0.003 ± 0.009

Table 11 *Seasonal and station wise variation of Chl-a, PSR during winter season (2018)*

Station	Season	Depth	CF (mg C/m2/day)	TC (mg/m3)	Chl-a (µg/l)	PSR (m/day)
Banshbaria	Winter	Surface-Bottom	3.68	1.95	0.21	1.89
Patenga	Winter	Surface-Bottom	7.77	3.04	0.46	2.56
Kutubdia	Winter	Surface-Bottom	2.12	4.16	0.16	0.48
Cox's Bazar	Winter	Surface-Bottom	1.15	2.89	0.24	0.36
Teknaf	Winter	Surface-Bottom	14.16	5.64	1.12	2.51

Table 12 *Seasonal and station wise variation of Chl-a, PSR during monsoon season (2018)*

Station	Season	Depth	CF (mg C/m2/day)	TC (mg/m3)	Chl-a (µg/l)	PSR (m/day)
Banshbaria	Monsoon	Surface-Bottom	5.59	2.13	0.21	2.63
Patenga	Monsoon	Surface-Bottom	8.24	3.58	0.69	2.3
Kutubdia	Monsoon	Surface-Bottom	1.41	4.82	0.06	0.29
Cox's Bazar	Monsoon	Surface-Bottom	2.35	5.62	0.29	0.42
Teknaf	Monsoon	Surface-Bottom	16.88	7.74	1.39	2.22

Table 13 *Seasonal and station wise variation of Chl-a, PSR during monsoon season (2023)*

Station	Season	Depth	Chl-a[µg/l]	CF[mg C/m2/day]	TC[mg/m3]	PSR[m/day]
Kutubdia	Winter	Surface-bottom	0.1	1.9	2.86	0.74
Cox's Bazar	Winter	Surface-bottom	0.22	2.42	4.55	0.5
Kutubdia	Pre-monsoon	Surface-bottom	0.08	2.65	6.85	0.32
Cox's Bazar	Pre-monsoon	Surface-bottom	0.41	1.08	3.44	0.33
Kutubdia	Monsoon	Surface-bottom	0.13	2.12	5.47	0.35
Cox's Bazar	Monsoon	Surface-bottom	0.15	2.41	5.3	0.57
Kutubdia	Post-monsoon	Surface-bottom	0.4	2	4.7	0.42
Cox's Bazar	Post-monsoon	Surface-bottom	0.78	1.27	4.75	0.27